Transgenic Mouse Models That Explore the Multistep Hypothesis of Intestinal Neoplasia

Steve H. Kim,*‡ Kevin A. Roth,*§ Amy R. Moser,‖ and Jeffrey I. Gordon*

Departments of *Molecular Biology and Pharmacology, ‡Surgery, and §Pathology, Washington University School of Medicine, St. Louis, Missouri 63110; and ‖McArdle Laboratory, University of Wisconsin, Madison, Wisconsin 53706

Abstract. SV-40 T antigen (TAg), human K-ras^{Val12}, and a dominant negative mutant of human p53 (p53^{Ala143}) have been expressed singly and in all possible combinations in postmitotic enterocytes distributed throughout the duodenal–colonic axis of 1–12-mo-old FVB/N transgenic mice to assess the susceptibility of this lineage to gene products implicated in the pathogenesis of human gut neoplasia. SV-40 TAg produces re-entry into the cell cycle. Transgenic pedigrees that produce K-ras^{Val12} alone, p53^{Ala143} alone, or K-ras^{Val12} and p53^{Ala143} have no detectable phenotypic abnormalities. However, K-ras^{Val12} cooperates with SV-40 TAg to generate marked proliferative and dysplastic changes in the intestinal epithelium. These abnormalities do not progress to form adenomas or adenocarcinomas over a 9–12-mo period despite sustained expression of the transgenes. Addition of p53^{Ala143} to enterocytes that synthesize SV-40 TAg and K-ras^{Val12} does not produce any further changes in proliferation or differentiation. Mice that carry one, two, or three of these transgenes were crossed to animals that carry *Min*, a fully penetrant, dominant mutation of the *Apc* gene associated with the development of multiple small intestinal and colonic adenomas. A modest (2–5-fold) increase in tumor number was noted in animals which express SV-40 TAg alone, SV-40 TAg and K-ras^{Val12}, or SV-40 TAg, K-ras^{Val12} and p53^{Ala143}. However, the histopathologic features of the adenomas were not altered and the gut epithelium located between tumors appeared similar to the epithelium of their single transgenic, bi-transgenic, or tri-transgenic parents without *Min*. These results suggest that (*a*) the failure of the dysplastic gut epithelium of SV-40 TAg X K-ras^{Val12} mice to undergo further progression to adenomas or adenocarcinomas is due to the remarkable protective effect of a continuously and rapidly renewing epithelium, (*b*) initiation of tumorigenesis in *Min* mice typically occurs in crypts rather than in villus-associated epithelial cell populations, and (*c*) transgenic mouse models of neoplasia involving members of the enterocytic lineage may require that gene products implicated in tumorigenesis be directed to crypt stem cells or their immediate descendants. Nonetheless, directing K-ras^{Val12} production to proliferating and nonproliferating cells in the lower and upper half of small intestinal and colonic crypts does not result in any detectable abnormalities.

THE mouse intestinal epithelium represents an attractive model system for examining how cellular proliferation, lineage allocation (commitment), and differentiation are normally regulated and how they are distorted during development of neoplasia. This is because proliferation and differentiation occur rapidly, continuously, and in a geographically well-organized fashion in this organ. The proliferative unit of the gut epithelium is the crypt of Lieberkühn. Each small intestinal and colonic crypt contains 350–500 cells (81) and is supplied by a single active multipotent stem cell functionally anchored near its base (30). The descendants of this stem cell undergo several rounds of cell division, creating a transit cell population. Approximately 60% of crypt epithelial cells pass through the cell cycle every 12 h (58). At some point during this series of amplifying divisions, cells are allocated to one of four lineages. The differentiation programs of these lineages are subsequently expressed during an orderly bipolar migration. In the small intestine, Paneth cells differentiate as they migrate to the base of each crypt where they reside for ~3 wk (11). Enterocytes, goblet, and enteroendocrine cells differentiate as they migrate upward in vertical, coherent bands from each monoclonal crypt to an adjacent villus (67). Once cells reach the apical extrusion zone of the villus, they are exfoliated into the gut lumen. Enterocytes, the principal epithelial cell lineage, complete their migration, differentiation/maturation, and exfoliation in 2–3 d (9, 81). Colonic crypts in adult mice, like small intestinal crypts, are monoclonal (31). The proliferative capacities of colonic and small intestinal crypts are similar (i.e., 6–21 new cells/h/crypt versus 12 cells/h/crypt) (73). Cells exit colonic crypts to a hexagonal-shaped cuff of surface epithelial cells which is the colonic homolog of the small intestinal villus (67).

A central question in gut epithelial cell biology is whether

expression of the differentiation programs of its various lineages is more dependent on cellular position along the crypt–villus (or crypt–surface epithelial cuff) axis or on the time that has elapsed since exiting the cell cycle. Studies of interspecies or heterotopic epithelial–mesenchymal recombinants suggest that reciprocal permissive and instructive interactions occur between fetal gut endoderm and mesoderm which can influence differentiation of epithelial cells (39–41). The importance of mesenchymal–stromal–epithelial cross talk in regulating the proliferation and/or differentiation programs of gut epithelial cell lineages in adult mice remains uncertain. However, the existence of such interactions could allow for maintenance of a lineage's differentiation program despite alterations in proliferation or in the rate of cell migration.

SV-40 T antigen (TAg)[1] and its mutant derivatives represent powerful tools for exploring the contribution of certain regulators of the cell cycle such as p53 and the retinoblastoma susceptibility gene product (pRB) to the proliferative state of a given cell lineage (8). A recent analysis of transgenic mice that carry intestinal fatty acid binding protein (I-FABP)/SV-40 TAg fusion genes indicated that initiation of transgene expression in postmitotic, villus-associated enterocytes results in their re-entry into the cell cycle (34). The nature of the cell cycle is different from that observed in crypts where the transgene is not expressed. DNA synthesis proceeds more slowly in differentiated villus-associated enterocytes. Villus enterocytes may also have difficulty passing through the G_2/M boundary (34).

Production of SV-40 TAg can be used to determine whether re-entry of enterocytes into the cell cycle changes their state of differentiation. Although analysis of the patterns of expression of several genes failed to disclose any such changes (34), migration and exfoliation of SV-40 TAg-producing enterocytes may occur too rapidly to allow dedifferentiation to occur or to be detected. Alternatively, the niche occupied by these cells (e.g., as defined by the underlying stroma and mesenchyme) may promote maintenance of the differentiated state and preclude dedifferentiation. We have explored these issues further by expressing gene products implicated in initiation and/or progression of human colonic neoplasia, singly and in various combinations, in villus-associated enterocytes. Analysis of these transgenic mice has provided information about the effects of these oncogenes on enterocytic proliferation/differentiation programs and about the requirements for progression of tumorigenesis in this organ.

Materials and Methods

Construction of FABP/Oncogene DNAs

Production of I-FABP$^{-1178\ to\ +28}$/SV-40 TAg (nucleotides 5235 to 2533) is described in Hauft et al. (34) (see Fig. 1 *A*).

L-FABP$^{-596\ to\ +21}$/K-ras^{Val12}, I-FABP$^{-1178\ to\ +28}$/K-ras^{Val12}, and I-FABP$^{-184\ to\ +28}$/K-ras^{Val12}. A 1.1-kb PstI–BamHI fragment, containing the coding sequence from the K-ras^{Val12} oncogene, was released from pSW11-1 (51). pLF/SV-40/Bluescript (33) contains nucleotides −596 to +21 of the rat liver fatty acid binding protein gene (*Fabpl*) (72) linked to a 0.9-kb fragment containing SV-40 early splice and late polyadenylation signals (26). The PstI–BamHI K-ras^{Val12} fragment from pSW11-1 was subcloned into the PstI site of pLF/SV-40/Bluescript using a BamHI–PstI oligodeoxynucleotide adapter (5′-GATCTGCA-3′), yielding pLF/K-ras^{Val12}/SV-40/Bluescript. L-FABP$^{-596\ to\ +21}$/K-ras^{Val12}/SV-40 was recovered from pLF/K-ras^{Val12}/SV-40/Bluescript as a 2.6-kb XhoI–SacI fragment (Fig. 1 *D*) and used for pronuclear injections. K-ras^{Val12}/SV-40 splice-polyadenylation DNA was recovered from pLF/K-ras^{Val12}/SV-40/Bluescript as a 2.0-kb BamHI fragment. A pBR325-based recombinant plasmid containing I-FABP$^{-1178\ to\ +28}$/SV-40 TAg (34) was digested with BamHI to excise the 2.7-kb coding sequence for SV-40 TAg. The K-ras^{Val12}/SV-40 BamHI fragment was subsequently ligated to BamHI-digested I-FABP$^{-1178\ to\ +28}$/pBR325 DNA, yielding pIF/K-ras^{Val12}/SV40/pBR325. I-FABP$^{-1178\ to\ +28}$/K-ras^{Val12}/SV-40 splice-polyadenylation DNA was retrieved as a 3.2-kb BspEI–BanI fragment (Fig. 1 *B*) for pronuclear injections. pIF/K-ras^{Val12}/SV-40/pBR325 was digested with BstEII and BsrFI. The 2.2-kb fragment released by these restriction enzymes (I-FABP$^{-184\ to\ +28}$/K-ras^{Val12}/SV-40 splice-polyadenylation; Fig. 1 *B*), was used for pronuclear injections.

I-FABP$^{-1178\ to\ +28}$/p53^{Wt} and I-FABP$^{-1178\ to\ +28}$/p53^{Ala143}. A 1.2-kb EcoRI–PstI fragment of pEPI-FABP (74), containing nucleotides −1178 to +28 of rat *Fabpi*, was subcloned into EcoRI–PstI digested pBluescript KS (Stratagene, LaJolla, CA). The *Fabpi* sequences were then excised using SalI and PstI. The resulting 1.2-kb SalI–PstI fragment was ligated to pLF/SV-40/Bluescript (after nucleotides −596 to +21 of rat *Fabpl* had been removed with SalI–PstI). This ligation created pIF/SV-40/Bluescript which placed the *Fabpi* promoter sequences upstream of the 0.9-kb fragment containing SV-40 splice/polyadenylation signals. A partial BamHI digest of the recombinant plasmid was performed since a second BamHI site was present at the 3′ end of the SV-40 sequence. Full-length, linearized DNA was isolated by agarose gel electrophoresis. A 1.8-kb fragment containing wild-type p53 cDNA (p53^{Wt}) was obtained by digesting pC53-SN3 (5) with BamHI. p53^{Wt} DNA was then ligated to linearized BamHI-digested pIF/SV-40/Bluescript. Correct orientation of the p53^{Wt} cDNA downstream from I-FABP$^{-1178\ to\ +28}$ and upstream from the SV-40 splice/polyadenylation sequences (Fig. 1 *C*) was confirmed by diagnostic restriction digests. I-FABP$^{-1178\ to\ +28}$/p53^{Ala143} was made by subcloning a 1.8-kb BamHI fragment of pC53-SCX3 (5) into pIF/SV-40/Bluescript. Both I-FABP$^{-1178\ to\ +28}$/p53^{Wt} and I-FABP$^{-1178\ to\ +28}$/p53^{Ala143} DNAs were released from vector sequences using HindIII and SpeI to give 4.0-kb fragments (Fig. 1 *C*) which were used for pronuclear injections.

Production of Transgenic Mice

All FABP/oncogene DNAs were purified by agarose gel electrophoresis followed by glass bead extraction (Geneclean II Kit; Bio 101 Inc., LaJolla, CA) and passage through a 0.2-μm Ultrafree MC Filter Unit (Millipore Corp., Bedford, MA). Each purified preparation of DNA was adjusted to a final concentration of 2 ng/μL TE buffer (10 mM Tris, 0.2 mM EDTA, pH 7.4). Pronuclear injections were performed using zygotes prepared from inbred FVB/N animals (Taconic Farms Inc., Germantown, NY). Injected eggs were transferred to pseudopregnant Swiss Webster females using standard techniques (36).

Live-born animals were screened for the presence of transgenes using the PCR, tail DNA, and the primers described in Fig. 1. Transgene copy number was determined by Southern blot hybridization analysis of BamHI-digested spleen DNA prepared from F_1 or F_2 mice. Blots were probed with a ^{32}P-labeled, 0.9-kb DNA containing the SV-40 splice/polyadenylation sequences present in every FABP/oncogene construct (see Fig. 1, *A–D*). Signal intensities produced by the DNAs from each pedigree were compared with signal intensities produced by known amounts of purified FABP/oncogene DNA included in each blot.

Members of FVB/N pedigrees with different FABP/oncogene DNAs were mated to produce multi-transgene mice. Tail DNA prepared from the progeny of these crosses was screened by PCR using primer pairs that were specific for each DNA construct and would amplify a different sized fragment (Fig. 1). This allowed us to use a single PCR reaction to perform a complete analysis of an animal's component transgenes.

Maintenance of Transgenic Mice

Transgenic mice and their normal littermates were maintained in microisolator cages under a strict light cycle (lights on at 0600 and off at 1800 h). Cages were changed in laminar flow hoods. Serologic studies confirmed that all mice used in this study were free of pathogens including murine hepatitis virus. Each transgenic pedigree was maintained by crosses to normal FVB/N littermates. Animals were given a standard autoclavable chow diet (No. 5010; Ralston Purina, St. Louis, MO) ad libitum. Transgenic mice and their normal littermates received an intraperitoneal injection of 5′-bromo-

1. *Abbreviation used in this paper*: TAg, T antigen.

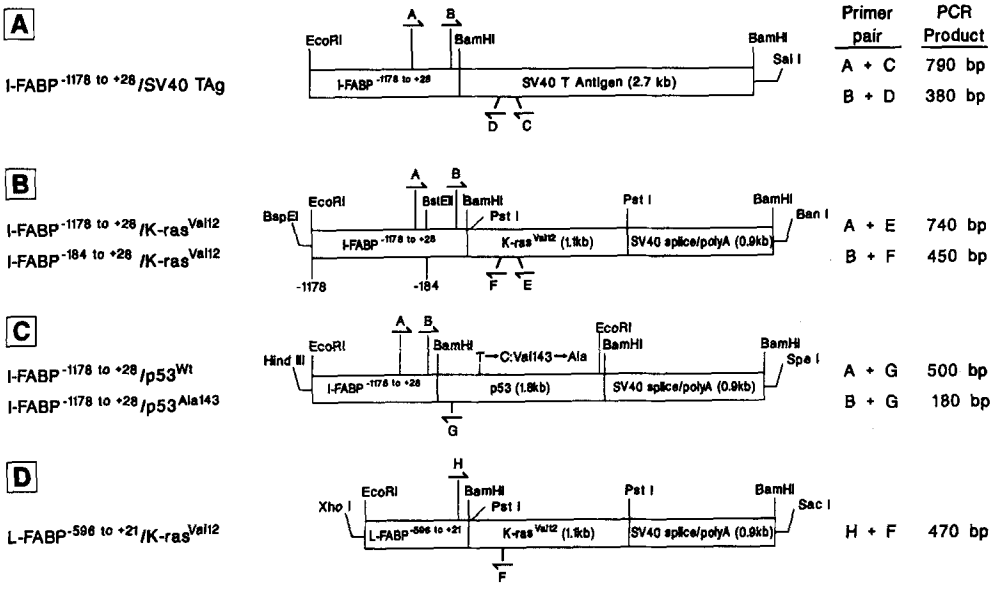

Figure 1. Schematic representation of FABP/oncogene constructs used to generate transgenic mice and the PCR assays used to establish their genotype. The following primers were used to genotype mice by PCR. Sense primers: (*A*) 5′-CCTTATTACAGCAGGCTAG-3′ (nucleotides −318 to −300 of rat *Fabpi*); (*B*) 5′-ATCTCTGCTTTCCTAGAGGCACACACAG-3′ (nucleotides + 1 to +28 of rat *Fabpi*); (*H*) 5′-CAGTGGGTGGCCTGGCAGACAG-3′ (nucleotides −25 to −4 of rat *Fabpl*). Antisense primers: (*C*) 5′-CATCCTCAGTAAGCACAGC-3′ (nucleotides 4790 to 4808 of the SV-40 genome); (*D*) 5′-TAAGGAAGAAGCAAATACCTCAGTTGCATCCCAG-3′ (nucleotides 4886 to 4919 of SV-40); (*E*) 5′-GCCTGTTTTGTGTCTACTGTTCTGGAAGGC-3′ (nucleotides 389 to 360 of exon 3 of K-ras); (*F*) 5′-GGACCATAGGCACATCTTCAGAGTCC-3′ (nucleotides 336 to 312 of exon 3 of K-ras); (*G*) 5′-ACTGCGGCTCCTCCATGGCAGTGACCCGGAAGGCAGTCTG-3′ (nucleotides 230 to 191 of exon 2 of p53).

deoxyuridine (BrdUrd; 120 mg/kg body weight) and 5′-flouro-deoxyuridine (12 mg/kg) 1.5 h before sacrifice to label cells in S-phase (15). All mice were killed by cervical dislocation.

Analysis of Regional and Cellular Patterns of Transgene Expression

The gastrointestinal tract was removed immediately after sacrifice and divided into eight segments—stomach (ST), duodenum (DU), proximal jejunum (PJ), distal jejunum (DJ), ileum (IL), cecum (CE), proximal colon (PC), and distal colon (DC)—according to a protocol described in Sweetser et al. (75). A 5-mm cross-sectional biopsy of each segment was recovered for histologic studies and fixed in Bouin's fluid. The remaining tissue from each small intestinal segment was weighed before RNA extraction. Colonic segments were not weighed due to marked animal-animal variations in the amount of luminal contents. Eight extra-intestinal tissues were also recovered for RNA isolation. These included brain, heart, lung, liver, spleen, pancreas, kidney, and skeletal muscle. Total cellular RNA was prepared from pulverized frozen tissues using the method of Chomczynski and Sacchi (12). The integrity of RNA preparations was assessed by denaturing agarose gel electrophoresis (63).

Tissue RNA was subjected to ribonuclease protection assays (63) to detect mRNA transcripts derived from transgenes and from endogenous mouse genes. SV-40 TAg mRNA was identified using a 178-base riboprobe (cRNA) derived from nucleotides 4886 to 5033 of the viral genome. The resulting protected sequence is 127 nucleotides long. A ^{32}P-labeled, 199-base cRNA yields a 148-base protected fragment when annealed to the mRNA transcript of I-FABP$^{-1178\text{ to }+28}$/k-ras^{Val12} (N.B. this protected fragment includes nucleotides 143 to 244 of human K-ras^{Val12} mRNA). The same cRNA produces a 54-base protected fragment when hybridized to mouse c-K-ras^{Gly12} mRNA. Production of wild-type and mutant p53 mRNAs was monitored using a 200-nucleotide riboprobe which spans exons 5 and 6 of the human p53 gene (5). This cRNA recognizes the products of the two I-FABP$^{-1178\text{ to }+28}$/p53 transgenes (Fig. 1 *C*) as a 150-base protected fragment and the mRNA product of the endogenous mouse p53 gene as an 80-base fragment. Expression of mouse *Fabpi* was assayed using a ^{32}P-labeled 562 base riboprobe. This cRNA generates a 501-nucleotide protected fragment when hybridized to nucleotides +121 to +621 mouse I-FABP mRNA. The mRNA products of the wild-type *Apc* gene and its mutant *Min* allele (*Apc*^{Min}) were measured using a 242-base cRNA which spans nucleotides 2527 to 2649 of Min cDNA (72). It yields a protected fragment of 123 bases when hybridized to Apc^{Min} mRNA and a protected fragment of 100 bases when hybridized to wild-type Apc mRNA. Polyacrylamide gels containing protected fragments were scanned with a radionuclide imager (Betagen, Waltham, MA). The intensity of the signal observed with each sample of tissue RNA was compared to the intensities of signals produced from known amounts of purified, in vitro transcribed, mRNA standards.

Bouin's fixed tissue samples were embedded in paraffin. 5-μm-thick sections were prepared and stained with hematoxylin and eosin or subjected to single or multilabel immunocytochemical analyses using protocols described in our previous publications (35, 61). The antisera used for these studies, their sources, final dilutions, and cell lineage specificities were as follows: goat anti-BrdUrd (1:1000–1:5000, references 13, 15; S-phase cells), rabbit anti-rat intestinal (I) -FABP (1:1000, reference 15; enterocytes), rabbit anti-rat liver (L) −FABP (1:1000, references 69, 75; enterocytes), rabbits anti-rat alkaline phosphatase (1:5000; reference 34; enterocytic lineage), rabbit anti-human lysozyme (1:500; reference 62; Paneth cell lineage), rabbit anti-serotinin (1:4000; Incstar Co., Stillwater, MN; subpopulation of the enteroendocrine lineage), and rabbit anti-substance P (1:2000; reference 60, subpopulation of the enteroendocrine lineage). Members of the goblet cell lineage were identified using the Periodic Acid Schiff (PAS) stain plus members of a panel of lectins with well defined carbohydrate specificities. SV-40 TAg was detected in Bouin's fixed sections with a rabbit anti-SV-40 TAg serum (1:2000; D. Hanahan, University of California, San Francisco) and in acetone-fixed frozen sections with a hamster antibody (1:1000; reference 34). Antigen-antibody complexes were visualized either with fluorescent-labeled second antibodies or with gold-labeled second antibodies and silver enhancement (35, 61).

Histopathologic Analysis of Gut Epithelium

A histological grading scheme was devised based on the pattern of BrdUrd staining observed along the crypt-villus (or crypt-surface epithelial cuff) axis and on the degree of dysplasia noted in hematoxylin and eosin stained sections: *0*, normal pattern of BrdUrd staining (S-phase cells limited to crypts) normal crypt-villus architecture; *1*, mild increase in BrdUrd labeling with extension of S-phase cells to the lower third of the villus—normal crypt-villus architecture; *2*, moderate increase in BrdUrd labeling extending to mid-villus; mild dysplasia; *3*, marked increase in BrdUrd labeling extending to upper third of the villus—moderate to severe dysplasia; *4*, adenoma; *5*, adenocarcinoma.

The proximal and distal halves of the small intestine (PSI and DSI, respectively) and the proximal half of the colon (PC) from each animal was surveyed by examining multiple cross sections of each segment or sections

prepared from Swiss rolls (31) of each region. All sections were evaluated in a single blinded fashion to minimize bias.

Analysis of Mice Carrying a Mutant Allele of the Murine Homolog of APC (Apc^{Min}) That Is Associated with Multiple Intestinal Neoplasms

C57Bl/6 *Min*/+ animals were re-derived by embryo transfer to assure ourselves that they were free of murine hepatitis virus. These animals, as well as the progeny of FVB/N X C57Bl/6 *Min*/+ or C57Bl/6 *Min*/+ X FVB/N I-FABP$^{-1178\ to\ +28}$/oncogene crosses, were identified as having a T→A transition in codon 850 of *Apc* (72) by PCR analysis of tail DNA. The 23-base upstream sense primer spanned nucleotides 2526 to 2549 of the *Min* allele's open reading frame and contained the mutated A residue at its 3' end (5'-CGTTCTGAGAAAGACAGAAGTTTA-3'). The antisense (downstream) primer spanned nucleotides 3065 to 3046 of the wild-type *Apc* sequence (5'-GGTGTATCCAGTTCTCCATC-3'). This primer pair only amplified the mutant *Min* allele, producing a 539-bp product.

Animals carrying *Min* were injected with BrdUrd 90 min before sacrifice. After animals were killed by cervical dislocation, their gastrointestinal tract was subdivided as described above. Each segment was then opened along its longitudinal axis and immediately fixed overnight in Bouin's solution. The number of intestinal neoplasms/segment was scored using a dissecting microscope. Segments were then rolled up and embedded in paraffin. 5–10-μm sections were prepared from these Swiss rolls and stained with hematoxylin and eosin or surveyed with our panel of antibodies.

Statistical Analysis

Statistical analysis of animal weights were performed by ANOVA using a P value of <0.05 as the cut-off for significance. Histopathologic scores were compared between single and multi-transgenic animals and their normal littermates using Fisher's Exact test with $P < 0.05$ considered to be statistically significant. SAS, version 6 (65) was used for these computations.

Results and Discussion

A large number of studies indicate that human colonic neoplasms arise from a multistep process. Initiation is thought to occur by somatic mutation of one or a small number of cells located in a single crypt (23). These mutations may affect the adenomatous polyposis coli (*APC*) gene, which is thought to function as a tumor suppressor (32,43) and/or the closely linked mutated in colorectal cancer gene (*MCC*) (44). The proposed consequence of these, or other, somatic mutations is to alter the proliferative potential of the initiated cell, leading to the development of small monoclonal adenomas. Subsequent progression appears to occur through a combination of mutational activation of proto-oncogenes and inactivation of tumor suppressor genes. These mutations frequently affect c-K-ras (7, 25, 80), the DCC (deleted in colorectal cancer) locus (24), and the p53 gene (4). Defects in the accuracy of DNA replication, controlled by a locus on human chromosome 2 (FCC), also appear to be associated with the development of hereditary nonpolyposis colorectal cancers and, possibly, sporadic colonic neoplasms (1, 57, 77).

We examined the effects of some of these gene products on gut epithelial differentiation/proliferation programs by expressing them singly and in combination in transgenic mice. Pedigrees of mice were initially established carrying nucleotides −1178 to +28 of the rat intestinal fatty acid binding protein gene (*Fabpi*; reference 74) linked to open reading frames encoding SV-40 TAg, K-ras^{Val12}, and p53^{Ala143}. I-FABP$^{-1178\ to\ +28}$ was selected because functional mapping studies conducted in transgenic mice had shown that it contains *cis*-acting elements which restrict expression of foreign gene products to nonproliferating members of the enterocytic lineage; i.e., reporter production is initiated just as enterocytes exit duodenal, jejunal, ileal and proximal colonic crypts. Expression is sustained as these cells complete their migration to the apical extrusion zone of villi or surface epithelial cuffs (15). Highest steady-state levels of reporter are encountered in the distal jejunal enterocytes with progressive declines occurring as one moves to the duodenum and to the proximal half of the colon (15). I-FABP$^{-1178\ to\ +28}$/reporter transgenes are activated on embryonic day 15/16, coincident with cytodifferentiation of the pseudostratified fetal gut epithelium to a monolayer overlying nascent villi. Expression is maintained along the duodenal–colonic axis for at least the first 12–14 mo of life. I-FABP$^{-1178\ to\ +28}$/oncogene transgenics were generated using inbred FVB/N zygotes (76) so as not to vary the genetic background when multiple oncogenes were introduced into a single mouse by pedigree crosses. We hoped that these initial studies would allow us to (*a*) define the proliferative potential of differentiating/differentiated villus-associated enterocytes, (*b*) determine whether enterocytes were capable of undergoing dedifferentiation in response to production of these gene products, and (*c*) ascertain if changes in proliferation/differentiation programs would progress; e.g., through clonal expansion of initiated cells and acquisition of subsequent somatic mutations.

Analysis of Mice with Single I-FABP$^{1178\ to\ +28}$/Reporter Transgenes

I-FABP$^{-1178\ to\ +28}$/SV-40 TAg. Two pedigrees of FVB/N I-FABP$^{-1178\ to\ +28}$/SV-40 TAg mice with 10–20-fold differences in the levels of SV-40 expression were studied (Table I). The pattern of I-FABP$^{-1178\ to\ +28}$/SV-40 TAg expression in 10–12-wk-old transgenic mice belonging to each pedigree mimicked that of the intact, endogenous mouse *Fabpi* gene (Fig. 2 *A*). Analysis of 1–12-mo-old F_1–F_3 mice from each line revealed that the concentration of SV-40 TAg mRNA in small intestinal and colonic RNA remained constant during the first year of life and that the transgene was not expressed in liver, kidney, pancreas, spleen, heart, lung, skeletal muscle, and brain (limits of detection = 0.01 pg SV-40 TAg mRNA/μg total cellular RNA).

Immunocytochemical surveys of mice belonging to the high expressing line 103 and the low expressing line 48 disclosed that SV-40 TAg is first detectable in enterocytes as they exit crypts. Transgene expression is sustained as these cells complete their upward migration to the apical extrusion zone of villi and to surface epithelial cuffs (e.g., Fig. 3, *A* and *C*). The distribution of SV-40 TAg along the crypt–villus axis is similar in animals belonging to lines 48 or 103. Only the intensity of nuclear staining is different, paralleling the differences in mRNA concentration (data not shown).

The effect of SV-40 TAg on cellular proliferation and differentiation was defined from the duodenum to the colon by (*a*) noting the distribution of cells in S-phase along the crypt–villus or crypt–surface epithelial cuff axis of mice that had been treated with BrdUrd 1.5 h before sacrifice; (*b*) surveying the number of villus-associated cells in M-phase in hematoxylin and eosin stained sections; (*c*) assessing whether there were any distortions of crypt–villus architecture or changes in cellular morphology; and (*d*) examining the expression of several lineage-specific gene products.

Line 103 mice between 8 and 210 d of age have numerous

Table I. Summary of Pedigrees of FVB/N Transgenic Mice

Transgene	No. of live-born animals	No. of transgenic founders	No. of expressing lines*	Expressing pedigree designation	Transgene copy no.
I-FABP$^{-1178\text{ to }+28}$/SV-40 TAg	103	2	2	48	5
				103	121
I-FABP$^{-1178\text{ to }+28}$/K-ras^{Val12}	96	12	5	24	4
				33	14
				57	ND
				73	53
				81	ND
I-FABP$^{-1178\text{ to }+28}$/p53^{Wt}	73	3	0	–	–
I-FABP$^{-1178\text{ to }+28}$/p53^{Ala143}	41	5	2	4	1
				14	1
I-FABP$^{-184\text{ to }+28}$/K-ras^{Val12}	89	3	1	65	ND
L-FABP$^{-596\text{ to }+21}$/K-ras^{Val12}	61	7	2	39	1
				44	1

* Defined by the presence of detectable levels of reporter mRNA in samples of jejunal RNA using a sensitive ribonuclease protection assay.

enterocytes in S-phase distributed from the base to the apex of duodenal, jejunal, and ileal villi (Fig. 3 *A*). M-phase cells are also present throughout the villus but are less numerous than S-phase cells (Fig. 3 *B*). Marked alterations in crypt–villus architecture are apparent, typically manifested by bizarre, branched villi (Fig. 3 *E*). These changes result in an average histopathologic grade of 2 in both the proximal and distal halves of the small intestine (Table II). This value is significantly different ($P < 0.001$) from values obtained from normal littermates. Modest proliferative abnormalities are also evident in the proximal half of the colon (average histopathologic grade = 1.3; Fig. 3, *C, D, and P*). The proliferative changes observed along the crypt–villus and duodenal–colonic axes of $G_0$103-derived mice are not associated with any detectable changes in the pattern of accumulation of L-FABP, I-FABP (Fig. 3 *F*), or alkaline phosphatase in enterocytes (data not shown). The differentiation programs of the three other principal gut epithelial cell lineages appears unperturbed, at least as operationally defined by our panel of antibodies and lectins and by light microscopic studies of cellular morphology (data not shown).

Surveys of hematoxylin and eosin stained sections prepared from Swiss rolls of small and large intestine failed to reveal any adenomas in 7–9-mo-old $G_0$103-derived mice. However, these animals often die of intestinal obstruction by 9 mo of age. This is due to large submucosal tumors in the proximal colon. These lesions are not apparent until 6–7 mo of age and are composed of SV-40 TAg-positive cells (Fig. 3 *G*). Transmission EM revealed nests and aggregates of neoplastic cells surrounded by a basal lamina (Fig. 3 *H*). The individual cells contain variable numbers of round, electron-dense, neurosecretory granules. The granules have a diameter of 100–200 nm and possess no obvious peripheral halo. These ultrastructural features are characteristic of a neuroendocrine cell neoplasm. There was no prior evidence that *Fabpi* or I-FABP$^{-1178\text{ to }+28}$/reporter transgenes are ex-

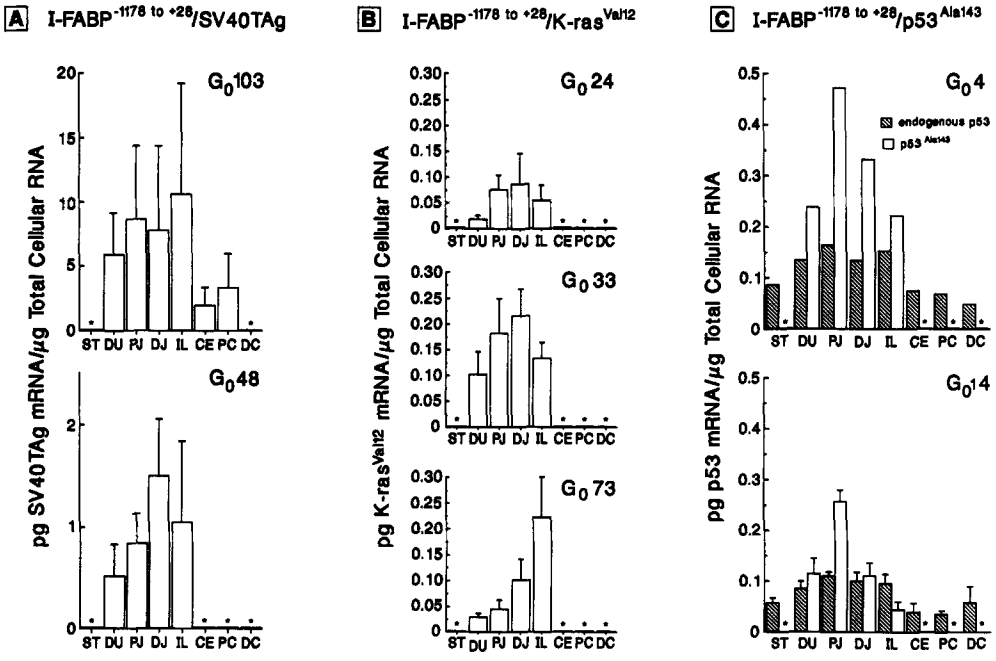

Figure 2. Regional patterns of expression of transgenes along the cephalocaudal axis of FVB/N mice. The steady state concentrations of reporter mRNAs were determined in 10–12-wk-old transgenic mice using ribonuclease protection assays (see Materials and Methods). The number of mice surveyed from each pedigree was as follows: (*A*) line 103, $n = 5$ mice; line 48, $n = 3$; (*B*) line 24, $n = 3$; line 33, $n = 3$, line 73, $n = 3$; (*C*) $G_0$4 was sterile; line 14, $n = 3$. *ST*, stomach; *DU*, duodenum; *PJ*, proximal jejunum; *DJ*, distal jejunum; *IL*, ileum; *CE*, cecum; *PC*, proximal colon; *DC*, distal colon (defined according to Sweetser et al. [75]). An asterisk indicates that the mRNA species was not detectable in RNA prepared from this segment.

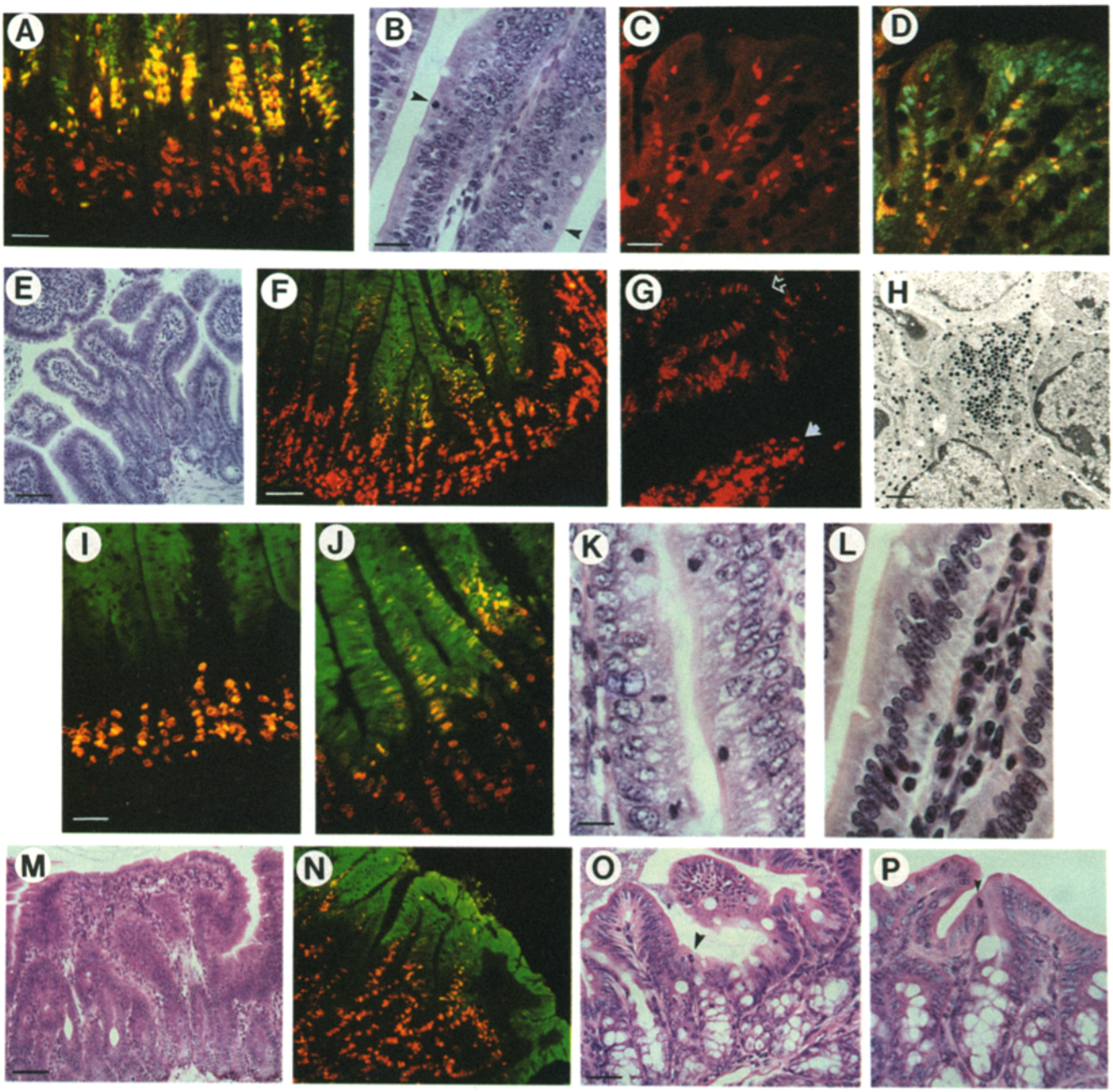

Figure 3. Analysis of the effects of SV-40 TAg and K-ras^{Val12} on the proliferation and differentiation programs of villus-associated enterocytes. SV-40 TAg and BrdUrd were detected in sections of jejunum or proximal colon with rabbit anti-SV-40 TAg and goat anti-BrdUrd sera. Antigen-antibody complexes were visualized using fluorescein-, also Cy3 Texas red-, or gold-labeled donkey anti-rabbit or anti-goat sera. (*A*) A section of jejunum from a 10-wk-old I-FABP$^{-1178\text{ to }+28}$/SV-40 TAg transgenic mouse belonging to the high expressing line 103 was incubated with antibodies directed against both BrdUrd and SV-40 TAg. BrdUrd-labeled nuclei in proliferating, crypt-associated cells do not contain detectable levels of SV-40 TAg and therefore appear red in this dual exposure photomicrograph. Cells containing both SV-40 TAg and BrdUrd are evident in the villus and appear yellow-orange. Nonproliferating, villus-associated enterocytes that contain SV-40 TAg appear green.(*B*) A hematoxylin- and eosin-stained section prepared from the jejunum of a 10-wk-old G_0 103-derived I-FABP$^{-1178\text{ to }+28}$/SV-40 TAg transgenic mouse reveals scattered villus-associated enterocytes in M-phase (*arrows*). (*C* and *D*) A section of proximal colon from an SV-40 TAg transgenic mouse belonging to line 103 was incubated with antibodies directed against BrdUrd (visualized with Texas red-labeled donkey anti-rabbit sera) and SV-40 TAg (visualized with gold-labeled donkey anti-rabbit serum followed by silver staining; photographed with reflected light polarization microscopy). S-phase cells are apparent in the upper third of these colonic crypts and their associated surface epithelial cuffs (*C*). SV-40 TAg production is evident in proliferating (*yellow-orange*) and nonproliferating (*aqua*) cells (*D*). (*E*) This hematoxylin- and eosin-stained section of jejunum illustrates the many dysplastic, branched villi encountered in 10–12-wk-old G_0 103-derived SV-40 TAg mice. (*F*) Despite these proliferative changes, the pattern of endogenous *Fabpi* expression remains unchanged in members of the high expressing SV-40 TAg pedigree. Dual labeling with rabbit anti-I-FABP serum (detected with fluorescein-labeled donkey anti-rabbit serum) and goat anti-BrdUrd serum discloses I-FABP (*green*) in villus-associated enterocytes in S-phase (*yellow-orange nuclei*). (*G*) G_0 103-derived I-FABP$^{-1178\text{ to }+28}$/SV-40 TAg mice develop large submucosal neoplasms in their proximal colon between 6 and 7 mo of age. The tumors consist of cells with high nuclear to cytoplasmic ratios, frequent mitotic figures, and a scant interlacing

Table II. Histopathologic Analysis of FVB/N Mice Carrying Single I-FABP$^{-1178\ to\ +28}$/Reporter Transgenes

Reporter	Pedigree	n	Age	Histologic grade* PSI	DSI	PC
–	Normal FVB/N	1	6 wk	0	0	0
		3	10–12 wk	0	0.3 ± 0.5	0.3 ± 0.5
		2	9 mo	0	0	0
SV-40 TAg	48	1	6 wk‡	1	1	0
		5	10–12 wk‡	0.6 ± 0.5	0.6 ± 0.5	0.2 ± 0.4
		1	9 mo‡	1	2	0
	103	3	10–12 wk	1.7 ± 0.5	2.3 ± 0.5	1.3 ± 0.5
		3	7 mo	2 ± 0	2.3 ± 0.5	1.3 ± 1.2
K-ras^{Val12}	24	1	6 wk	1	1	0
		2	10–12 wk	0	0.5 ± 0.5	0.5 ± 0.5
		1	9 mo	0	0	0
	33	2	10–12 wk	0	0.5 ± 0.5	0.5 ± 0.5
		1	9 mo	0	0	0
	73	3	10–12 wk	0	0 ± 0	0 ± 0
		1	9 mo	0	0	0
p53^{Ala143}	4	1	19 wk	0	1	0
	14	4	10–12 wk	0.25 ± 0.4	0.25 ± 0.4	0.25 ± 0.4
		1	28 wk	0	0	1

* The histologic grading system used to score each segment is described in Materials and Methods.
‡ Analysis of six nontransgenic littermates, 6; 10–12, and 36 wk of age revealed scores of zero in each of these segments.
n, number of animals scored; *PSI*, proximal half of small intestine; *DSI*, distal half of small intestine; *PC*, proximal colon.

pressed in small intestinal or colonic enteroendocrine cell populations (15). The late appearance of proximal colonic endocrine neoplasms in this pedigree suggests that SV-40 TAg may only be produced in a small subset of enteroendocrine cells. "Initiated," SV-40 TAg-positive colonic enteroendocrine cells may be more likely to progress to dysplasia and neoplasia since their turnover time (23 d; reference 79) is considerably slower than the turnover times of small intestinal enteroendocrine cells (4 d; reference 10) (e.g., transgenic mice carrying nucleotides −2100 to +58 of the rat glucagon gene linked to SV-40 TAg exhibit no detectable abnormalities in their small intestinal endocrine cell populations but develop focal areas of colonic enteroendocrine hyperplasia that progress to invasive plurihormonal endocrine neoplasms by the end of the fourth postnatal week) (48).

Mice from the low-expressing line 48 contain far fewer villus-associated enterocytes in S-phase than age-matched animals from line 103 and have essentially no changes in crypt–villus architecture (Table II). Their colonic epithelium appears normal. They have no detectable abnormalities in the differentiation program of their villus- and surface-epithelial cuff associated neuroenterocytes (Fig. 4 and data not shown) nor do they have any neoplasms, including the endocrine tumors seen in the proximal colon of line 103 mice.

I-FABP$^{-1178\ to\ +28}$/K-ras^{Val12}. 12 transgenic founders carrying I-FABP$^{-1178\ to\ +28}$/K-ras^{Val12} were identified among 96 live-born mice screened (Table I). Ribonuclease protection analysis of jejunal RNA prepared from F_1 animals revealed that five pedigrees expressed the transgene (Table I). Levels of K-ras^{Val12} mRNA in 10–12-wk-old animals from each of the three lines we studied were markedly lower than SV-40 TAg mRNA (Fig. 2, *A* and *B*). The regional pattern of I-FABP$^{-1178\ to\ +28}$/K-ras^{Val12} expression along the duodenal–colonic axis was generally similar to that of *Fabpi* (Fig. 2 *B*). K-ras^{Val12} mRNA was not detectable in RNA prepared from the stomach, colon, or 8 extraintestinal tissues in any of the lines studied (Fig. 2 *B* and data not shown).

K-ras^{Val12} expression in postmitotic villus-associated enterocytes produces no significant phenotypic abnormalities.

stroma. Enterocytes in the overlying colonic epithelium (*open arrows*) as well as the neoplasm's poorly differentiated cells (*closed arrows*) contain SV-40 TAg (*G*). (*H*) EM examination of glutaraldehyde-fixed tumor shows nests and groups of neoplastic cells surrounded by a basal lamina. The cells contain numerous, round, electron-dense, neurosecretory granules at their periphery. These ultrastructural features are characteristic of a neuroendocrine cell neoplasm. (*I*) In contrast to the pedigrees carrying I-FABP$^{-1178\ to\ +28}$/SV-40 TAg, I-FABP$^{-1178\ to\ +28}$/K-ras^{Val12} transgenic mice have no detectable abnormalities in the proliferation or differentiation programs of their enterocytes. This is illustrated by the normal pattern of BrdUrd and I-FABP staining along the crypt–villus axis of the jejunum in a 10-wk-old animal. (*J–N*) When I-FABP$^{-1178\ to\ +28}$/K-ras^{Val12} mice are crossed to I-FABP$^{-1178\ to\ +28}$/SV-40 TAg animals, the resulting bi-transgenic progeny exhibit proliferative and cytologic abnormalities in their villus epithelium. Comparison of high magnification photomicrographs of hematoxylin and eosin sections of jejunum prepared from a 10-wk-old bi-transgenic mouse (*K*) and a comparably aged normal FVB/N animal (*L*) underscores the marked increases in mitotic activity, in nuclear pleomorphism, and in nuclear–cytoplasmic ratios. (*M* and *N*) Despite the marked distortions in crypt–villus architecture (*M*) and the proliferative changes which occur in SV-40 TAg X K-ras^{Val12} bi-transgenic mice, *Fabpi* expression appears to be sustained in their villus-associated enterocytes (*N*). G_0 103-SV-40 TAg X G_0 73 K-ras^{Val12} mice have a hyperplastic and dysplastic proximal colonic epithelium (*O*) compared to their SV-40 TAg parent (*P*). Bars: (*A–C*, *I*, and *O*) 25 μm; (*E*, *F*, and *M*) 50 μm; (*H*) 1 μm; (*K*) 10 μm.

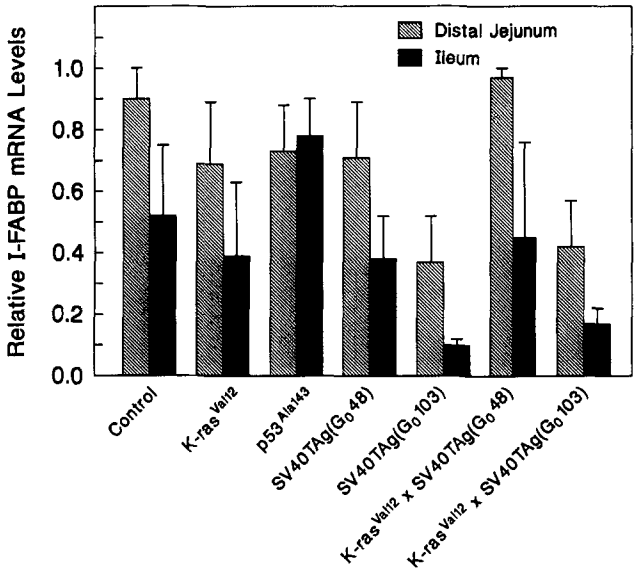

Figure 4. Effect of I-FABP$^{-1178\ to\ +28}$/oncogene transgenes on steady-state levels of I-FABP mRNA in the small intestine of young adult FVB/N mice. A ribonuclease protection assay was used to determine the concentration of I-FABP mRNA in total cellular RNA prepared from the distal jejunum and ileum of transgenic mice. I-FABP mRNA levels are expressed relative to levels observed in the distal jejunum of nontransgenic littermates. Values shown for I-FABP$^{-1178\ to\ +28}$/K-ras^{Val12} transgenics were determined from animals belonging to lines 24, 33, and 73 (n = ten 10–12 wk-old mice). Three 10–12-wk-old I-FABP$^{-1178\ to\ +28}$/p53^{Ala143} mice from pedigree 14 were surveyed. At least three 10–12-wk-old mice were examined from each of two SV-40 TAg-producing pedigrees and from each of the two types of SV-40 TAg X K-ras^{Val12} crosses.

BrdUrd-positive cells are not present in small intestinal villi (Fig. 3 *I*). There are no villus-associated enterocytes in M-phase and there are no distortions in crypt–villus architecture (Table II). Extensive immunocytochemical surveys in 1–9-mo-old mice from each of the three pedigrees did not reveal any perturbations in the differentiation programs of any of the four gut epithelial cell lineages (Figs. 3 *I* and 4; and data not shown). No tumors were seen in 9-mo-old mice even though I-FABP$^{-1178\ to\ +28}$/K-ras^{Val12} is still expressed at levels comparable with that encountered at 1–3 mo of age.

I-FABP$^{-1178\ to\ +28}$/p53^{Ala143} and I-FABP$^{-1178\ to\ +28}$/p53^{Wt}. p53 is thought to play an important role in regulating cellular proliferation, differentiation, and survival: (*a*) effects on the cell cycle have been demonstrated in normal and transformed cells (5, 6, 18, 38, 45, 49, 52, 68, 71); (*b*) it can regulate the activities of a variety of promoters, including those that may be needed for ongoing cell proliferation (21, 22, 27, 28, 42); and (*c*) p53 may function as a "guardian" of the genome by affecting DNA repair in response to injury (38, 45). p53 mRNA is distributed along the length of the duodenal–colonic axis of young adult FVB/N mice. Highest steady-state concentrations occur in the proximal and distal jejunum (Fig. 2 *C*). We were unable to detect any p53 along the crypt–villus or crypt–surface epithelial cuff axis of adult FVB/N mice using commercially available antibodies. In addition, we know of no report describing the pattern of accumulation of this protein or its mRNA along this axis in adult mice. (In situ hybridization studies of E18.5 mouse intestine have shown that steady-state p53 mRNA levels are higher in cells located in the intervillus epithelium [the precursor to crypts] than in cells overlying nascent villi [66].)

To examine the role of p53 in regulating the proliferation potential and differentiation program of villus-associated enterocytes, we generated mice with transgenes encoding either wild-type human p53 (p53^{wt}) or a dominant negative mutant human protein (p53^{Ala143}). 5 out of 41 live born mice surveyed contained I-FABP$^{-1178\ to\ +28}$/p53^{Ala143} (Table I). $G_0$4 was sterile and was sacrificed at 19 wk of age. Expression of the transgene was seen in the expected gut-specific pattern with highest levels in the proximal jejunum (Fig. 2 *C*). A pedigree was established from $G_0$14. Its F_1 progeny also expressed the transgene along the length of the duodenal–ileal axis with highest levels in the proximal jejunum (Fig. 2 *C*). Ribonuclease protection assays indicated that the molar ratio of human p53^{Ala143} mRNA to mouse p53^{Wt} mRNA was 2:1 in the proximal small intestine of members of this pedigree (Fig. 2 *C*). We could not identify any abnormalities in gut epithelial proliferation or differentiation programs in these mice (Table II and data not shown). Founder $G_0$4 had no apparent phenotypic abnormalities affecting enterocytes or any of the other intestinal epithelial cell lineages even though the steady state level of mutant p53 mRNA was three fold higher than mouse p53^{Wt} mRNA in duodenum and proximal jejunum.

Three transgenic founders with I-FABP$^{-1178\ to\ +28}$/p53^{Wt} were identified (Table I). Two passed the transgene to their progeny. None of these mice had detectable levels of wild-type human p53 mRNA in intestinal or extraintestinal tissues when surveyed at 10–12 wk of age (limits of detection ~0.01 pg p53^{Wt} mRNA/μg total cellular RNA). Male G_0^{51} failed to pass the transgene to 20 F_1 progeny and did not have detectable p53^{Wt} mRNA in either small intestine, colon, or any of the eight extraintestinal tissues included in our survey. Our inability to identify lines of mice that produce detectable levels of human p53^{Wt} mRNA may be because p53^{Wt} overexpression in the gut causes lethality or it may simply reflect the effect of sequences flanking the site of insertion of the transgene (see reference 46 for a discussion of difficulties encountered in expressing certain p53 variants in transgenic mice).

Analysis of Mice That Express Two or More Oncoproteins in Villus-associated Enterocytes Reveals That SV-40 TAg and K-ras^{Val12} Cooperate to Affect Proliferation/Differentiation

SV-40 TAg binds to and inactivates p53 as well as the retinoblastoma susceptibility gene product (pRB), a tumor suppressor that regulates progression through the cell cycle (16, 19, 29). Members of FVB/N I-FABP$^{-1178\ to\ +28}$/SV-40 TAg pedigrees that express high and low levels of the reporter were crossed to FVB/N mice that produced K-ras^{Val12} and/or p53^{Ala143} so that we could determine whether enterocytes are responsive to these oncoproteins during their residence on the villus. Ribonuclease protection assays of jejunal and ileal RNAs established that (*a*) the concentrations of SV-40 TAg, K-ras^{Val12}, and p53^{Ala143} mRNA in mice carrying two or three different transgenes were comparable to levels observed in their single or bi-transgenic parents and (*b*) these mRNAs did not undergo any appreciable time-dependent

Table III. Histopathologic Analysis of FVB/N Mice Carrying Two or Three Transgenes

Transgenic crosses	n	Age	Histologic Grade* PSI	DSI	PC
SV-40 TAg (48) × K-ras^{Val12} (73)	1	10 wk	1	2	1
SV-40 TAg (48) × K-ras^{Val12} (33)	2	11 wk	1.5 ± 0.5	1.5 ± 0.5	1.5 ± 0.5
	3	9 mo	2 ± 0	1.7 ± 0.5	0.5 ± 0.5
SV-40 TAg (48) × K-ras^{Val12} (24)‡	2	11.5 wk	0.5 ± 0.5	0.5 ± 0.5	0.5 ± 0.5
SV-40 TAg (103) × K-ras^{Val12} (73)	1	6 wk	2	2	ND
	2	10 wk	1.5 ± 0.5	2.5 ± 0.5	2 ± 1
	5	7 mo	2.6 ± 0.5	3 ± 0	2.2 ± 0.4
SV-40 TAg (103) × K-ras^{Val12} (24)	1	12 wk	2	3	2
SV-40 TAg (48) × p53^{Ala143} (14)	2	12 wk	2 ± 0	1 ± 0	0.5 ± 0.5
SV-40 TAg (103) × p53^{Ala143} (14)	1	7 wk	1	1	1
	2	10 wk	1.5 ± 0.5	2.5 ± 0.5	1.5 ± 0.5
K-ras^{Val12} (73) × p53^{Ala143} (14)	2	10–12 wk	0 ± 0	1 ± 0	0.5 ± 0.5
SV-40 TAg (103) × K-ras^{Val12} (73) × p53^{Ala143} (14)	1	3 wk	1	2	2
	1	6 wk	2	2	1
	2	10 wk	2 ± 0	3 ± 0	2 ± 0

Pedigree numbers are indicated in parentheses.
* See Materials and Methods for a description of the grading system used to score each segment.
‡ The importance of SV-40 TAg and K-ras^{Val12} mRNA levels in determining these phenotypic changes is illustrated from the results obtained after crossing members of the low expressing line of SV-40 TAg mice to the K-ras^{Val12} pedigree with the lowest steady state level of reporter mRNA (line 24; see Fig. 2 *B*). The resulting bi-transgenic progeny have the same phenotype as their $G_0$48-derived SV-40 TAg parents (see Table II).
Abbreviations are defined in Table II.

changes in their steady-state levels over a 6–40-wk period (data not shown).

As noted above, mice from the low expressing SV-40 TAg line have minimal phenotypic abnormalities in their enterocytic population. However, when they are crossed to $G_0$33- or $G_0$73-derived K-ras^{Val12} animals, histopathologic scores in the proximal small intestine of their bi-transgenic offspring increase significantly when compared to age matched littermates carrying either I-FABP/SV-40 TAg or I-FABP/K-ras^{Val12} alone ($P<0.05$, respectively; see Table III). These changes are evident at the earliest time points surveyed (4–6 wk) and are sustained throughout the next 6–9 mo of life. However, histopathologic scores in the proximal colon of the bi-transgenic mice are not significantly different from either single transgene-containing parents or age matched normal FVB/N mice – likely reflecting the absence of detectable levels of both SV-40 TAg and K-ras^{Val12} mRNAs in this portion of the gut (see Fig. 2, *A* and *B*).

Bi-transgenic animals obtained from crossing members of the high expressing SV-40 TAg line (line 103) to either of the high expressing K-ras^{Val12} lines (pedigrees 33 or 73) exhibit marked proliferative and dysplastic changes in their small intestinal and colonic epithelium. S- and M-phase cells are evident along the length of the villus (Fig. 3, *J* and *K*). The nuclear–cytoplasmic ratio in proliferating and nonproliferating enterocytes is increased and cells with nuclear hyperchromatism and atypia are evident (Fig. 3, compare *K* and *L*). The normal architecture of the crypt–villus axis is greatly perturbed. Numerous branched villi are present as are anaplastic polyploid structures (Fig. 3, *M* and *N*). These hyperplastic changes are associated with significant increases in the relative weight of the small intestine (Fig. 5). $G_0$103 SV-40 TAg X K-ras^{Val12} mice also have significantly different ($P < 0.001$) histopathologic scores in their proximal colon compared to normal, age-matched FVB/N mice (Table III). S- and M-phase cells are present in the upper portions of colonic crypts and their associated surface epithelial cuffs. There are pronounced increases in the cellularity of the surface epithelial cuff and alterations in the nuclear-to-cytoplasmic ratio of enterocytes (Fig. 3, compare *O* and *P*). Like the proliferative and morphologic changes observed in the small intestine, the colonic abnormalities are apparent at the earliest time point sampled (postnatal weeks 4–6) and do not progress during the next 9 mo of life. Co-expression of K-ras^{Val12} and SV-40 TAg does not affect the time of appear-

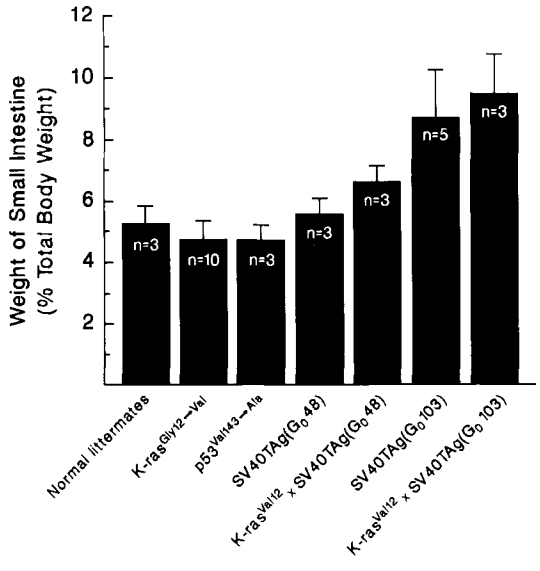

Figure 5. Effect of I-FABP$^{-1178\ to\ +28}$/oncogene transgenes on the relative weight of small intestine in adult FVB/N mice. See Materials and Methods for further details.

ance or the phenotype of the proximal colonic endocrine tumors (data not shown).

These findings suggest that villus-associated enterocytes can support cooperative interactions between oncoproteins (37) during their rapid transit along the crypt–villus axis. Since G_0 103 SV-40 TAg X $G_0$73 K-ras^{Val12} bi-transgenic mice demonstrate the most dramatic changes in proliferation and tissue architecture when compared to their single transgene-containing parents, they were mated to $G_0$14-derived-p53^{Ala143} animals to determine whether the dominant negative p53 mutant produced progression of these abnormalities. We could not detect any differences in proliferative activity in the small intestinal or colonic epithelium of these tri-transgenic offspring and their bi-transgenic parents at 10 wk of age, even though the steady state levels of SV-40 TAg and K-ras^{Val12} mRNAs were comparable in all mice (Table III and data not shown). Immunocytochemical surveys of the duodenal–colonic axis of bi-transgenic and tri-transgenic mice failed to disclose any changes in the differentiation programs of Paneth cell, goblet cell, or enteroendocrine cell lineages (data not shown). Despite the marked changes in morphology of proliferating and nonproliferating duodenal, jejunal, and ileal enterocytes, they contain readily detectable levels of I-FABP, L-FABP, and alkaline phosphatase. Moreover, the fact that these cells are SV-40 TAg-positive provides functional evidence that they produce a constellation of transcription factors necessary to support expression of I-FABP$^{-1178\ to\ +28}$ (and *Fabpi*; see Fig. 4). Bi- and tri-transgenic mice grow at the same rate as normal FVB/N mice and subsequently maintain body weights from 3–9 mo of age that are not significantly different from normal nontransgenic or single transgene-containing animals (data not shown). This finding provides further support for the conclusion that functional maturation of enterocytes is not disrupted by production of these oncoproteins. Finally, none of the bi-transgenic or tri-transgenic mice examined developed intestinal adenomas or adenocarcinomas over a 6–9-mo period.

Two control experiments were performed to examine the mechanisms that may produce the phenotypic changes observed in villus-associated enterocytes of SV-40 TAg X K-ras^{Val12} mice. First, $G_0$48 SV-40 TAg mice were crossed to p53^{Ala143} animals. Addition of the mutant p53 produced only minimal differences in the phenotype induced by SV-40 TAg: histopathologic scores in the proximal small intestine of 10-wk-old bi-transgenic mice were only slightly higher than in 10-wk-old $G_0$48 SV-40 TAg animals (Table III; P = 0.05) while no differences in histopathologic scores were noted in their distal small intestine or in their proximal colon (Table III). Second, p53^{Ala143} mice were crossed to $G_0$73 K-ras^{Val12} animals. Unlike the cooperative effects observed between ras and mutant p53 in other epithelial cell lineages (e.g., prostate) (50), villus enterocytes that coexpress mutant p53^{Ala143} and K-ras^{Val12} without SV-40 TAg show no significant phenotypic abnormalities when compared with enterocytes in comparably aged, normal FVB/N mice (Table III and data not shown). It is possible that the dysplastic changes in villus-associated enterocytes produced by addition of K-ras^{Val12} to SV-40 TAg-positive enterocytes could be due to their reduced functional pools of mouse p53. Such reductions could allow K-ras^{Val12} to produce "unopposed" dedifferentiation of proliferating enterocytes. This concept is supported by the observation that p53^{Ala143} is necessary for maintenance of the phenotype of ras-transformed rat embryo fibroblasts (82). If this hypothesis is true, p53^{Ala143}'s failure to cause progression of the dysplasia observed in SV-40 TAg/K-ras^{Val12} positive enterocytes may be due to the fact that it cannot produce further reductions in functional mouse p53 pools other than what is already achieved by SV-40 TAg (see reference 54). Other possibilities include differences in the distributions of wild-type mouse and mutant human p53 along the crypt–villus axis and/or the inability of the mutant human protein to produce a dominant negative effect via interaction with nascent mouse p53 synthesized in enterocytes [53]). The importance of SV-40 TAg-mediated inactivation of mouse p53^{Wt} in allowing K-ras^{Val12} to exert its effect on enterocytes can be tested in at least two ways. SV-40 TAg deletion mutants which lack the ability to bind p53 and/or Rb (8, 70) could be expressed in this cell lineage alone, and in combination with K-ras^{Val12} and/or p53^{Ala143}. I-FABP/K-ras^{Val12} mice could also be crossed to mice that are homozygous for p53 null mutations (20).

Is Gut Neoplasia Initiated in the Crypt Stem Cell or One of Its Immediate Descendants?

Cellular differentiation is generally viewed as a loss of proliferation potential. Our analysis of mice with one or more I-FABP$^{-1178\ to\ +28}$/oncogene transgenes indicates that differentiated, villus-associated enterocytes are capable of re-entering the cell cycle and undergoing dedifferentiation. The lack of progression of the dysplastic changes noted in SV-40 TAg X K-ras^{Val12} bi-transgenic animals, or in SV-40 TAg X K-ras^{Val12} X p53^{Ala143} tri-transgenic mice suggests that the products of these transgenes are not sufficient to support functional anchorage of villus-associated enterocytes and that these cells are unable to acquire additional somatic mutations required for progression, even over a 9–12-mo period. The inability of these cells to undergo further progression emphasizes (*a*) the remarkable protective effect produced by a continuously and rapidly renewing epithelium; (*b*) the need to identify gene products that may affect cell migration rates along the crypt–villus axis and lead to functional anchorage of initiated cells; and (*c*) the need to use other transcriptional regulatory elements to direct production of these oncoproteins to crypt epithelial cell populations: specifically the functionally anchored stem cell or one of its immediate descendants (17). With these thoughts in mind, we generated several additional lines of transgenic mice to determine the consequences of initiating K-ras^{Val12} production in the crypt.

Analysis of I-FABP$^{-184\ to\ +28}$ and L-FABP$^{-596\ to\ +21}$/K-ras^{Val12} Mice. Removal of nucleotides −1178 to −185 from I-FABP$^{-1178\ to\ +28}$/reporter transgenes does not affect developmental, cell lineage-specific, or cephalocaudal patterns of reporter production (15). However, precocious activation of transgene expression occurs in proliferating and nonproliferating cells located in the middle and upper thirds of duodenal, jejunal, ileal, and proximal colonic crypts (15). Expression is sustained in members of the enterocytic lineage as they complete their migration from the crypt to the apical extrusion zones of villi. Nucleotides −596 to +21 of the homologous rat liver fatty acid binding protein gene can also be used to direct foreign gene expression to proliferating

and nonproliferating cells located in duodenal, jejunal, ileal, proximal, and distal colonic crypts (69, 75). However, reporter production is initiated in the lower third of crypts, closer to the presumed stem cell zone than is observed with I-FABP$^{-184\ to\ +28}$ (69). Moreover, L-FABP$^{-596\ to\ +21}$/reporter transgenes are expressed in all four gut epithelial cell lineages as they migrate along the crypt–villus (and -surface epithelial cuff) axis (61, 78). L-FABP$^{-596\ to\ +21}$/reporter transgenes are activated at the same time in fetal development as I-FABP$^{-1178\ to\ +28}$/reporter and I-FABP$^{-184\ to\ +28}$/reporter transgenes (E15/E16) and expression is maintained at constant levels in small intestine, proximal colon, hepatocytes, and proximal renal tubular epithelial cells during the first 6–9 mo of life (14, 69). In contrast, I-FABP$^{-184\ to\ +28}$ expression decreases several fold during the weaning period (15).

We chose to examine the effects of K-ras^{Val12} in the crypt in view of previous conclusions that ras-mediated alterations in the differentiation programs of other epithelial cell lineages requires a proliferating population of target cells (2, 3, 47). Three lines of I-FABP$^{-184\ to\ +28}$/K-ras^{Val12} mice were established (Table I). None of the transgenic mice belonging to these pedigrees appeared to have any abnormalities in the proliferation and differentiation programs of their gut epithelial cells at 4–8 wk of age (data not shown). Subsequent ribonuclease protection studies of small intestinal and colonic RNA prepared from 1-d-old animals indicated that only members of pedigree 65 contain detectable levels of K-ras^{Val12} mRNA. By postnatal day 10 (P10), the concentration of this mRNA falls markedly to the point where it is barely detectable. Neither P1 nor P10 mice belonging to line 65 have demonstrable phenotypic abnormalities in their gut epithelium when compared to their nontransgenic littermates. Thus, progressive extinction of I-FABP$^{-184\ to\ +28}$/reporter expression limits its usefulness in exploring the consequences of K-ras^{Val12} expression in proliferating and nonproliferating crypt epithelial cells.

Two pedigrees of L-FABP$^{-596\ to\ +21}$/K-ras^{Val12} transgenic mice were also studied (Table I). The founders, $G_0$39 and 44, became moribund at 15 and 13 wk of age, respectively. Biochemical analysis of their serum obtained at the time of sacrifice indicated that they were suffering from renal failure ([blood urea nitrogen] >10 times normal) and had hepatocellular damage without cholestasis (alanine aminotransferase and aspartate aminotransferase activities were >20 times normal while alkaline phosphatase activity and bilirubin concentration were within normal limits). Their kidneys appeared pale, nodular, and slightly enlarged. Multiple proximal tubular epithelial cells in S-phase were readily apparent in these animals (Fig. 6 *A*) but not in their comparably aged normal littermates. The proximal tubules and collecting ducts were markedly dilated. Glomerulosclerosis was evident (Fig. 6 *B*). The liver was enlarged three fold in both founders. There were mild dysplastic changes in hepatocytes (Fig. 6 *C*). Scattered members of this lineage were in S-phase (Fig. 6 *D*). In contrast, there were no apparent proliferative abnormalities in the gut epithelium. BrdUrd-positive cells were restricted to the crypt and crypt–villus architecture appeared entirely normal (Fig. 6 *E*). Moreover, there were no detectable perturbations in the morphology or differentiation programs of the four principal gut epithelial cell lineages (for example see Fig. 6 *F*). The transgenic progeny of $G_0$39 and 44 became moribund by postnatal week 8–12 and exhibited histopathologic changes in their liver and kidney which were indistinguishable from those noted in their transgenic parents. Their small intestinal and colonic epithelium appear normal. Ribonuclease protection studies confirmed that the expression domain of L-FABP$^{-596\ to\ +21}$/K-ras^{Val12} along the cephalocaudal axis of the gut resembled that of other L-FABP$^{-596\ to\ +21}$/reporter transgenes (69, 75).

The inability of K-ras^{Val12} to produce detectable changes in the biological properties of proliferating crypt epithelial cells or in the differentiation programs of their enterocytic, goblet, Paneth, or enteroendocrine cell descendants, contrasts with the sensitivity of the hepatocyte and renal tubular epithelial cell lineages to this (or other) mutant ras protein (see reference 64). The apparent resistance of proliferating and nonproliferating gut epithelial cell populations may reflect (*a*) the absence of signaling pathways which can be perturbed by K-ras^{Val12}, (*b*) the presence of gene products which oppose K-ras^{Val12}-mediated changes in proliferation/differentiation (e.g., p53), and/or (*c*) the inability of initiated, K-ras^{Val12}-producing crypt (and villus) cells to be retained for a sufficient period so that this oncoprotein can produce detectable effects – either by itself or after the acquisition of additional somatic mutations. Possibilities *b* and *c* can be explored by mating mice containing L-FABP$^{-596\ to\ +21}$/K-ras^{Val12} to mice containing L-FABP$^{-596\ to\ +21}$ linked to other oncogenes (e.g., SV-40 TAg and its mutant derivatives) or to mice that are homozygous for p53 null alleles.

Analysis of Min/+ Mice That Carry One or More Transgenes. As noted above, APC mutations apparently occur early in the multistep journey to human colorectal neoplasia and are thought to be important for initiation (59). A Leu→Stop mutation in codon 850 of the C57Bl/6 mouse *Apc* gene is associated with the development of multiple intestinal adenomas (55, 56, 72). C57Bl/6 *Min*/+ mice first develop adenomas during the fifth postnatal week. 100–120-d-old animals exhibit striking differences in the number of tumors along their duodenal–colonic axis with highest concentrations present in the distal jejunum and ileum (Fig. 7 *A*). Adenomas are rarely found in the colon[2] (Fig. 7 *A*). This regional variation in tumor number contrasts with the constant levels of Apc and Apc^{Min} mRNAs from the stomach to the distal colon (Fig. 7 *B*). *Min*/+ mice generally die by postnatal day 140 from anemia due to persistent intestinal bleeding (Fig. 7 *C*). We found that *Min* adenomas contain small foci of differentiated enterocytes, Paneth, goblet, and enteroendocrine cells (56). Expression of endogenous marker genes in these differentiated cells is appropriate for the position that these lineages occupy along the duodenal–colonic axis. The presence of multiple lineages/adenoma, each with an appropriate "positional address," suggests that tumorigenesis in *Min*/+ mice may be initiated through a stochastic process in

2. Intestinal tumors are observed in animals as young as 5 wk of age in the colony of B6 *Min*/+ mice maintained in Madison. The average number of tumors for 100–120-d-old animals in this colony is 24 ± 7 for the small intestine and 5 ± 4 for the colon using the scoring method described by Moser et al. (55). The highest number of adenomas occur in the proximal small bowel (55, 56). Mice rederived and maintained in St. Louis develop fewer tumors at 100–120 d of age: 17 ± 6 in small intestine; 4 ± 2 in colon using the scoring method of Moser et al. (55). The highest concentrations of adenomas occur in the distal jejunum and ileum. These colonies differ with respect to viral status and diet. The factors responsible for these observed differences in *Min* phenotype have not yet been identified.

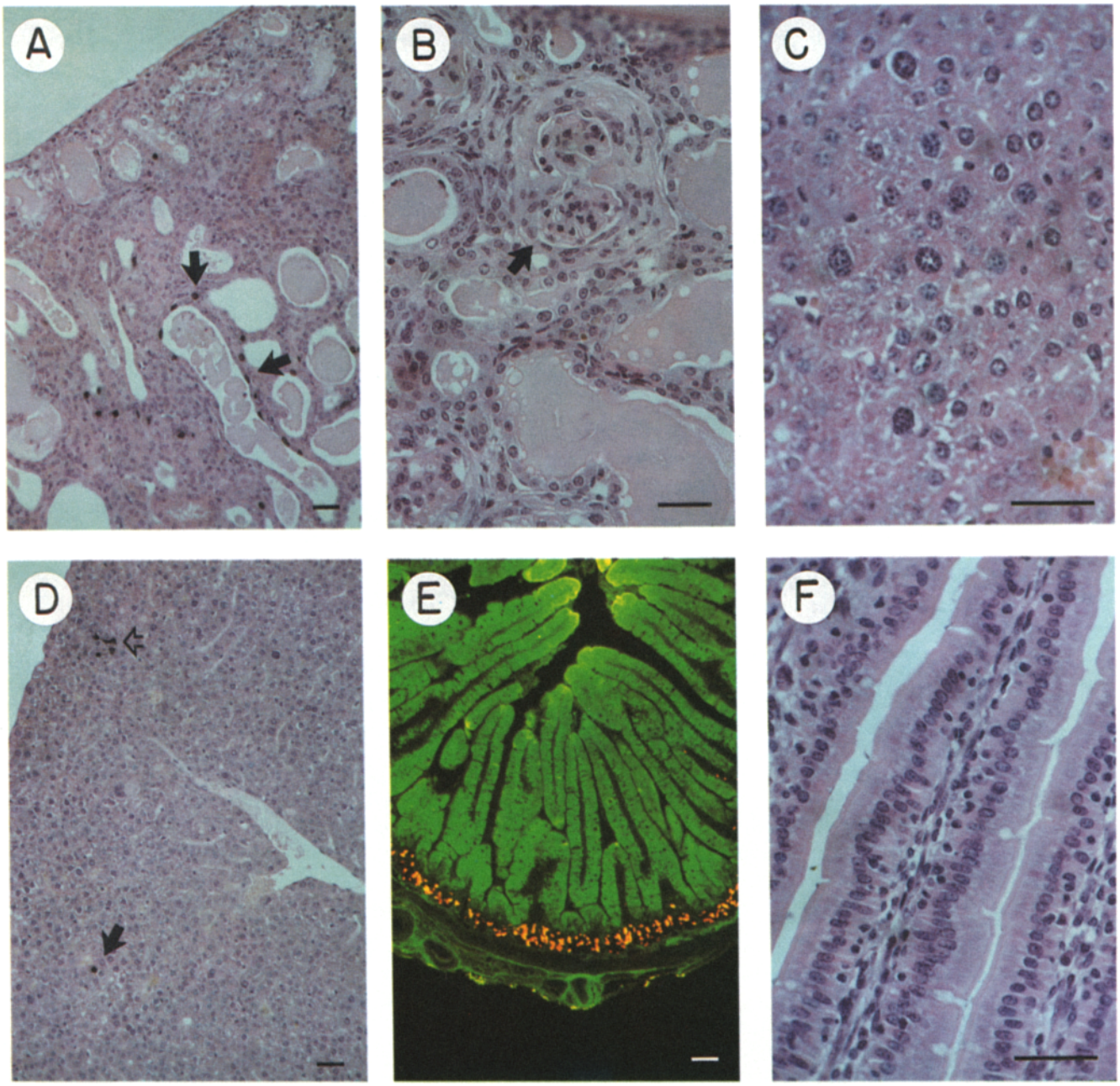

Figure 6. Analysis of 10–12-wk-old L-FABP$^{-596\ to\ +21}$/K-ras^{Val12} transgenic mice. (*A*) Section of kidney showing several BrdUrd-labeled cells in the proximal tubular epithelium (detected with goat anti-BrdUrd serum and IGSS; *arrows*). Many tubules and collecting ducts are grossly dilated and filled with proteinaceous material. Moderate interstitial fibrosis and focal chronic inflammation are present. There is no evidence of significant dysplasia. (*B*) A sclerotic glomerulus is indicated by the arrow. Glomeruli show varying degrees of sclerosis, from minor segmental damage to diffuse hyalinization. (*C* and *D*) Hematoxylin- and eosin-stained sections of liver show a hypercellular parenchyma. Hepatocytes exhibit increased nuclear–cytoplasmic ratios, decreased cytoplasmic glycogen, increased nuclear atypia, and moderate pleomorphism (*C*). BrdUrd staining in *D* reveals scattered cells in S-phase (indicated by a closed arrow) as well as small clusters of proliferating hepatocytes (*open arrow*). No frankly neoplastic foci are evident. (*E* and *F*) Sections of proximal jejunum show no obvious proliferative abnormalities. Double labeling of the section in *E* with rabbit anti–L-FABP and goat anti-BrdUrd sera (detected with fluorescein-labeled donkey anti–rabbit and Cy3–labeled donkey anti–goat antibodies, respectively) demonstrates that BrdUrd positive cells (*orange*) are restricted to crypt while L-FABP (*green*) is confined to villus-associated enterocytes. High power view of intestinal villi in *F* shows normal appearing enterocytes and goblet cells. No villus-associated epithelial cells are seen in M-phase. Bars, 25 μm.

the multipotent crypt stem cell or one of its immediate descendants (56).

Min adenomas do not progress unless mice are crossed to other strains (e.g., AKR/J or MA/MyJ) that contain unlinked modifier alleles. The resulting hybrid mice have fewer tumors, a longer lifespan (up to 300 d), and develop foci of adenocarcinoma in their adenomas late in life—likely reflecting the acquisition of additional somatic mutations required for progression (e.g., loss of heterozygosity).

We introduced *Min* into the genomes of our FVB/N trans-

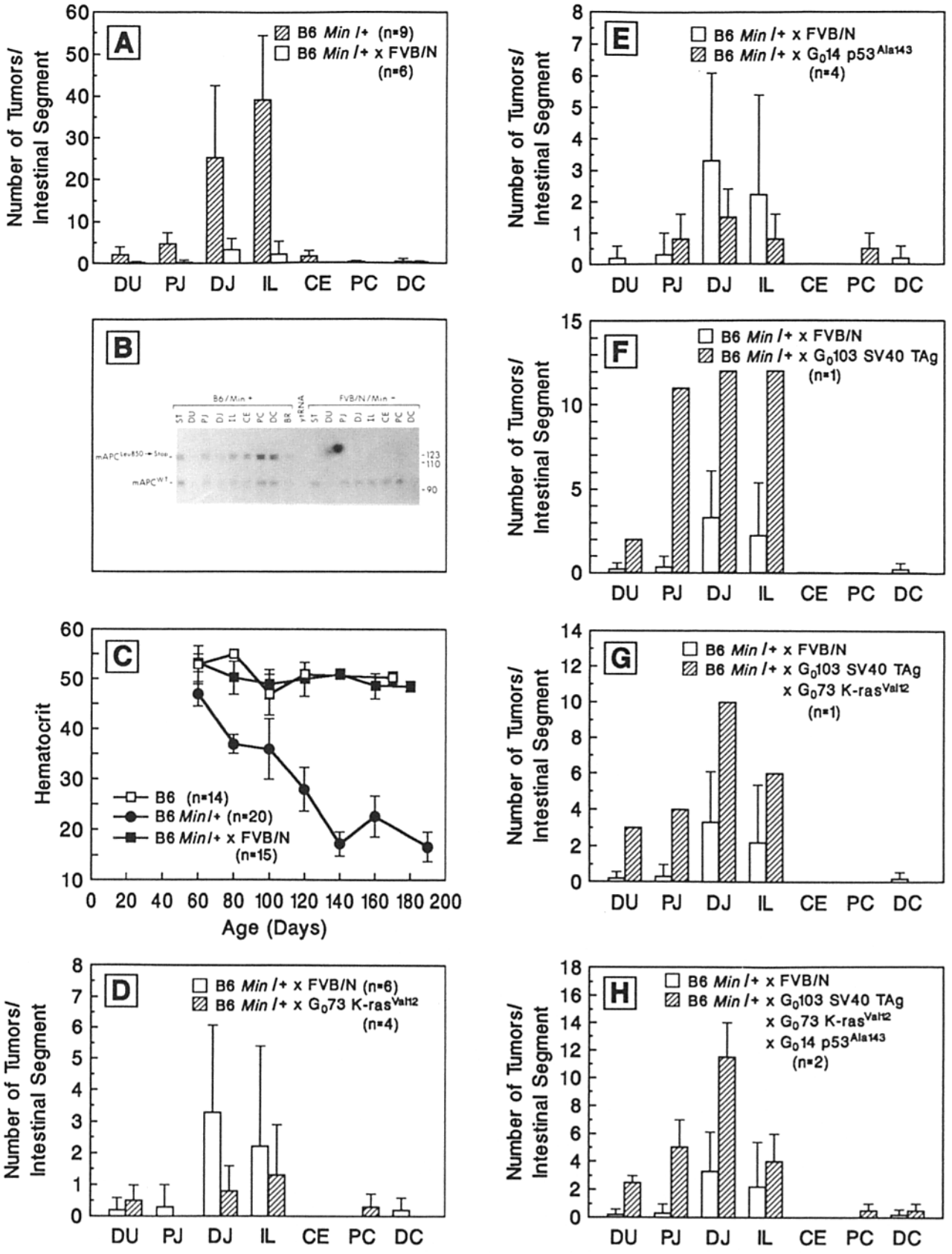

Figure 7. Effect of I-FABP$^{-1178\text{ to }+28}$/oncogene transgenes on the number and distribution of intestinal adenomas in *Min*/+ mice. The number of adenomas was determined along the cephalocaudal axis of the gut in 100–120-d-old mice using procedures described in Materials and Methods. The number of mice surveyed is indicated in parentheses. *B* shows the distribution of Apc and Apc^{Min} mRNAs along the cephalocaudal axis of the intestine of normal FVB/N and C57Bl/6 *Min*/+ mice as determined by a ribonuclease protection assay (see Materials and Methods). Additional abbreviations used include: *BR*, brain; *ytRNA*, yeast tRNA. The positions of migration of MspI DNA fragments derived from pBR322 are shown to the right of the figure. (*C*) Hematocrits were determined on samples of blood recovered by retro-orbital phlebotomy at various ages (n = 14 C57Bl/6 mice; 20 C57Bl/6 *Min*/+ mice; and fourteen C57Bl/6 *Min*/+ X FVB/N animals). (*D–H*) Effect of I-FABP$^{-1178\text{ to }+28}$/oncogene transgenes on tumor number in 100–120-d-old mice that carry *Min*.

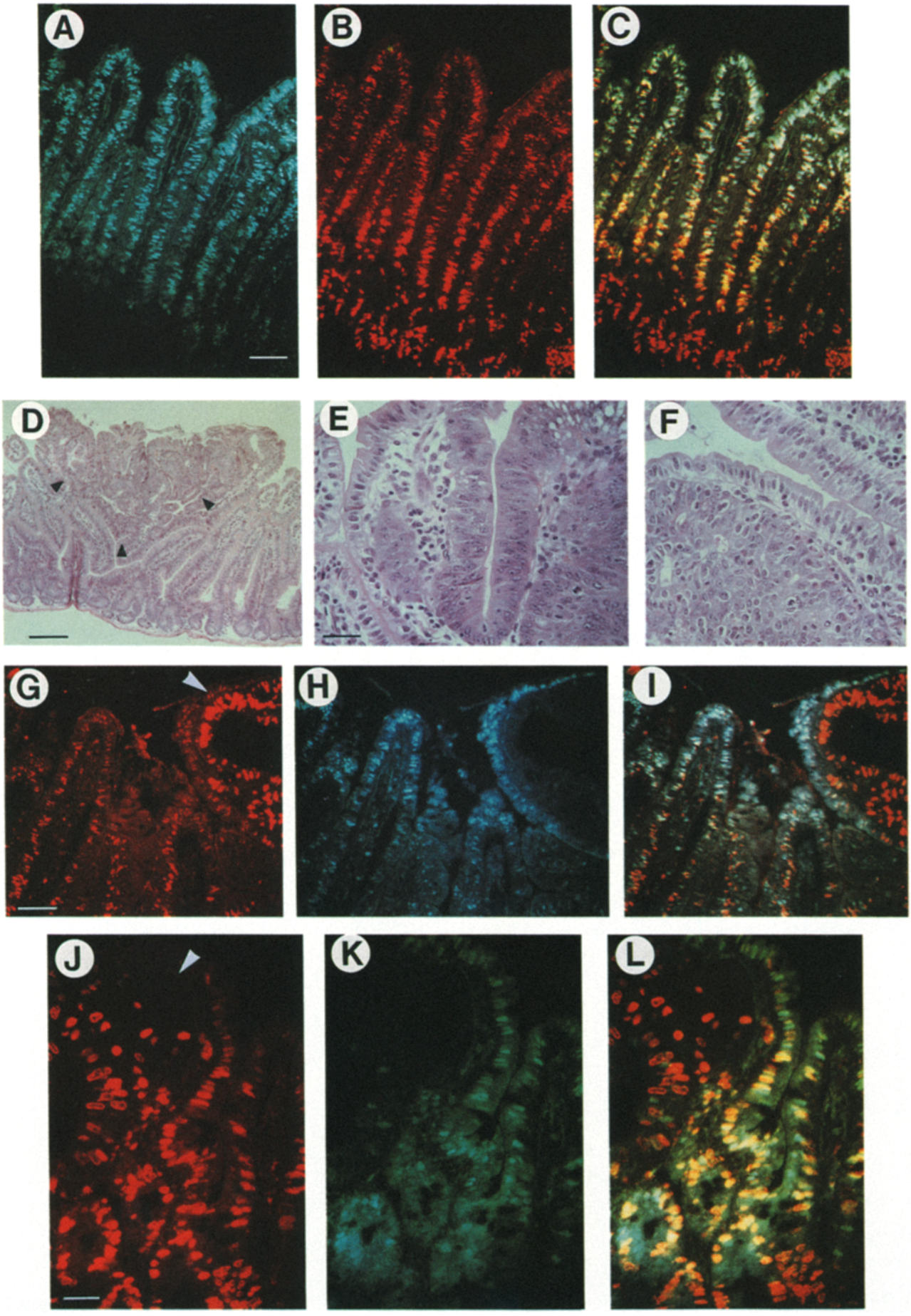
A
B
C
D
E
F
G
H
I
J
K
L

genic mice to assess the role of its protein product on enterocytic proliferation, migration, and differentiation programs and to determine if it could cause progression of the dysplasia encountered in initiated, villus-associated enterocytes. An initial control experiment confirmed that *Min* is fully penetrant in FVB/N X C57Bl/6 *Min*/+ mice. However, the number of tumors is at least an order of magnitude lower in their distal jejunum and ileum (Fig. 7 *A*), suggesting the presence of at least one modifier allele in the FVB/N genome (but not necessarily the same one as in AKR or MA). The cephalocaudal variation in tumor number observed in these hybrid mice resembles the variation noted in their C57Bl/6 *Min*/+ parent (Fig. 7 *A*). The reduction in overall tumor number is associated with a reduction in intestinal blood loss and increased lifespan (to >200 d; see Fig. 7 *C*). The intestinal adenomas of 90–180-d-old FVB/N X *Min*/+ C57Bl/6 hybrids have the same histological features as the adenomas of comparably aged *Min*/+ C57Bl/6 animals (data not shown).

Min/+ C57Bl/6 mice were crossed to members of SV-40 TAg line 103 or K-ras^{Val12} line 73 or p53^{Ala143} line 14. They were also mated to mice carrying two transgenes ($G_0$103 SV-40 TAg X $G_0$73 K-ras^{Val12}), and to mice carrying three transgenes ($G_0$103 SV-40 TAg X $G_0$73 K-ras^{Val12} X $G_0$14 p53^{Ala143}). Animals from each cross (n = 1-4) were sacrificed between postnatal days 100 and 120. The epithelium located between intestinal neoplasms appeared similar to the epithelium of the parental single transgene-containing, bi-transgenic, or tri-transgenic mice without *Min* (e.g., compare Fig. 8, *A–C* with Fig. 3 *A*). There are several possible explanations for the failure of *Min* to produce progression of the dysplasia noted in SV-40 TAg/K-ras^{Val12} positive enterocytes. First, the expression of domains of *Min* and the transgenes may not overlap along the crypt–villus axis, e.g., Apc and Apc^{Min} may be confined to the crypt or not expressed in enterocytes. Second, the dysplastic changes induced by SV-40 TAg and K-ras^{Val12} may repress *Apc*/*Apc*^{Min} expression in villus-associated enterocytes. Third, the residence time of these villus-associated cells may be too short for the mutant protein to exert its effect(s). Fourth, the villus' enterocytic population may not possess the metabolic machinery necessary to support whatever further changes this mutant protein could potentially produce in their proliferation/differentiation programs.

No significant increase in average tumor numbers occurs in *Min* X K-ras^{Val12} or *Min* X p53^{Ala143} mice (control group = comparably aged FVB/N X *Min*/+ C57Bl/6 animals housed under identical conditions; Fig. 7, *D* and *E*). When *Min* is introduced into the genomes of mice carrying I-FABP$^{-1178\ to\ +28}$/SV-40 TAg, or into the genomes of the bi-transgenic and tri-transgenic animals, tumor number increases 2–3-fold in the distal jejunum and ileum and 2–5-fold in the duodenum/proximal jejunum. No significant changes are detectable in the cecum or colon (Fig. 7, *F–H*). Remarkably, the distribution of tumors along the duodenal–colonic axis is similar to the distribution in mice with *Min* alone.

The phenotypes of intestinal adenomas in 100–120-d-old *Min* X K-ras^{Val12} or *Min* X p53^{Ala143} or *Min* X SV-40 TAg mice are indistinguishable from the phenotypes of adenomas in control 100–120-d-old FVB/N X C57Bl/6 *Min*/+ animals (data not shown). The phenotypes of adenomas in 100–120-d-old *Min* X SV-40 TAg X K-ras^{Val12} mice and *Min* X SV-40 TAg X K-ras^{Val12} X p53^{Ala143} mice (e.g., Fig. 8, *D–F*) are also similar to the phenotype of adenomas in control hybrid animals. Tumors in mice carrying I-FABP$^{-1178\ to\ +28}$/SV-40 TAg do not have detectable levels of SV-40 TAg in their proliferating and nonproliferating cell populations (Fig. 8, *G–L*), suggesting that the degree of differentiation of these cells is not sufficient to allow I-FABP$^{-1178\ to\ +28}$ to function.

The observation that I-FABP$^{-1178\ to\ +28}$/SV-40 TAg plus I-FABP$^{-1178\ to\ +28}$/K-ras^{Val12} only produce a small increase in the number of jejunal/ileal adenomas provides independent support for the hypothesis that initiation of tumorigenesis in *Min* mice is a stochastic event which typically occurs in crypts rather than in villus-associated epithelial cell populations. Since Apc/Apc^{Min} mRNA levels are constant along the cephalocaudal axis of the gut, the observed modest increase in tumor number without a change in their duodenal–colonic distribution is consistent with the notion that initiated cells in *Min*/+ mice must acquire additional somatic mutations to progress to adenomas and that cells located in the distal half of the mouse small intestine are more vulnerable to these mutations than those in the colon. The dysplastic epithelium of our bi-transgenic and tri-transgenic mice may contribute to this enhanced vulnerability and/or to help promote progression during the early stages of tumorigenesis. The absence of detectable progression in Min X transgene adenomas once they form may be due to the fact that their poorly differentiated cellular populations are unable to support I-FABP$^{-1178\ to\ +28}$-mediated transcription of

Figure 8. Analysis of the effect of I-FABP$^{-1178\ to\ +28}$/oncogene transgenes on the gut epithelium of *Min*/+mice. (*A–C*) 120-d-old mouse carrying I-FABP/SV-40 TAg + I-FABP/K-ras^{Val12} + I-FABP/p53^{Ala143} and *Min*. SV-40 TAg (detected as aqua-colored material using rabbit anti-SV-40 TAg serum, gold-labeled donkey anti-rabbit antibodies, and silver intensification staining) is present in both crypt and villus-associated epithelial cells (*A*). Re-entry of villus-associated enterocytes into the cell cycle is indicated in *B* by the numerous red-appearing BrdUrd-labeled cells (detected with goat anti-BrdUrd serum and Texas red–labeled second antibodies). Double exposure clearly illustrates the presence of BrdUrd and SV-40 TAg in the orange-colored nuclei of villus-associated enterocytes. (*D*) Hematoxylin and eosin stained section of jejunum demonstrates an adenoma (*arrow*) arising within the hyperplastic and dysplastic intestinal epithelium typical of a 120-d-old mouse carrying *Min* plus the three transgenes. (*E* and *F*) Higher magnification views of hematoxylin and eosin-stained jejunal sections prepared from the mouse shown in *D* demonstrate that the adenoma is composed of cells which are more dysplastic than those which populate the epithelium located between tumors. (*G–L*) I-FABP$^{-1178\ to\ +28}$/ does not function in the poorly differentiated cells of an adenoma present in a *Min*/+ X SV-40 TAg X K-ras^{Val12} X p53^{Ala143} mouse. *G* and *J* show frequent BrdUrd-labeled cells in both adenomas (*arrows*) and in the intervening non-adenomatous epithelium. *H* and *K* show numerous SV-40 TAg-labeled nuclei in non-adenomatous villus epithelium and only rare, weakly stained nuclei in the adenomas. Dual exposure in *I* and *L* demonstrates the relationship between SV-40 TAg expression and BrdUrd labeling in non-adenomatous epithelium. The ability of this epithelium to support production of SV-40 TAg in its proliferating and nonproliferating cell populations contrasts with the lack of detectable SV-40 TAg in the adjacent adenoma. Bars: (*A* and *G*) 50 μm; (*D*) 100 μm; (*E* and *J*) 25 μm.

oncogenes (Fig. 8, *G–L*). In contrast, L-FABP$^{-596\ to\ +21}$ may support reporter production in Min adenomas. If so, crossing *Min* mice to transgenic animals containing one or more L-FABP$^{-596\ to\ +21}$/oncogene DNAs may allow reconstitution of a multistep process that ultimately leads to development of intestinal adenocarcinoma.

We are indebted to David O'Donnell for his help in maintaining lines of transgenic mice, Bert Vogelstein for generously supplying us with cDNAs encoding human p53^{Wt} and p53^{Ala143}, William F. Dove for his critical reading of this manuscript and Lawrence Creswell for his help with statistical analysis.

This work was supported by grants from Glaxo and from the National Institutes of Health (DK30292, CA50585, CA23076, and CA07075).

Received for publication 26 May 1993 and in revised form 21 July 1993.

References

1. Aaltonen, L. A., P. Peltomäki, F. S. Leach, P. Sistonen, L. Pylkkänen, J.-P. Mecklin, H. Järvinen, S. M. Powell, J. Jen, S. R. Hamilton, G. M. Petersen, K. W. Kenzler, B. Vogelstein, and A. de la Chapelle. 1993. Clues to the pathogenesis of familial colorectal cancer. *Science (Wash. DC).* 236:812–816.
2. Andres, A. C., O. Bchini, B. Schubaur, B. Dolder, M. LeMeur, and P. Gerlinger. 1991. H-*ras* induced transformation of mammary epithelium is favoured by increased oncogene expression or by inhibition of mammary regression. *Oncogene.* 6:771–779.
3. Bailleul, B., M. A. Surani, S. White, S. C. Barton, K. Brown, M. Blessing, J. Jorcano, and A. Balmain. 1990. Skin hyperkeratosis and papilloma formation in transgenic mice expressing a *ras* oncogene from a suprabasal keratin promoter. *Cell.* 62:697–708.
4. Baker, S. J., E. R. Fearon, J. M. Nigro, S. R. Hamilton, A. C. Preisinger, J. M. Jessup, P. van Tuinen, D. H. Ledbetter, D. F. Barker, Y. Nakamura, R. White, and B. Vogelstein. 1989. Chromosome 17 deletions and p53 gene mutations in colorectal carcinomas. *Science (Wash. DC).* 244:217–221.
5. Baker, S. J., S. Markowitz, E. R. Fearon, J. K. V. Willson, and B. Vogelstein. 1990. Suppression of human colorectal carcinoma cell growth by wild-type p53. *Science (Wash. DC).* 249:912–915.
6. Bischoff, J. R., P. N. Friedman, D. R. Marshak, C. Prives, and D. Beach. 1990. Human p53 is phosphorylated by p60-cdc2 and cyclin B-cdc2. *Proc. Natl. Acad. Sci. USA.* 87:4766–4770.
7. Bos, J. L., E. R. Fearon, S. R. Hamilton, M. Verlaan-de Vries, J. H. van Boom, A. J. van der Eb, and B. Vogelstein. 1987. Prevalence of *ras* gene mutations in human colorectal cancers. *Nature (Lond.).* 327:293–297.
8. Chen, J., G. J. Tobin, J. M. Pipas, and T. Van Dyke. 1992. T-antigen mutant activities *in vivo*: Roles of p53 and pRB binding in tumorigenesis of the choroid plexus. *Oncogene.* 7:1167–1175.
9. Cheng, H., and C. P. LeBlond. 1974. Origin, differentiation and renewal of the four main epithelial cell types in the mouse small intestine. I. Columnar cells. *Am. J. Anat.* 141:461–480.
10. Cheng, H., and C. P. LeBlond. 1974. Origin, differentiation and renewal of the four main epithelial cell types in the mouse small intestine. III. Enteroendocrine cells. *Am. J. Anat.* 141:503–520.
11. Cheng, H,. and C. P. Leblond. 1974. Origin, differentiation and renewal of the four main epithelial cell types in the mouse small intestine. IV. Paneth cells. *Am. J. Anat.* 141:521–536.
12. Chomczynski, P., and N. Sacchi. 1987. Single-step method of RNA isolation by acid guanidinium thiocyanate-phenol-chloroform extraction. *Anal. Biochem.* 162:156–159.
13. Cohn, S. M., and M. W. Lieberman. 1984. The use of antibodies to 5'-bromo-2'deoxyuridine for the isolation of DNA sequences containing excision-repair sites. *J. Biol. Chem.* 259:12456–12462.
14. Cohn, S. M., K. A. Roth, E. H. Birkenmeier, and J. I. Gordon. 1991. Temporal and spatial patterns of transgene expression in aging adult mice provide insights about the origins, organization and differentiation of the intestinal epithelium. *Proc. Natl. Acad. Sci. USA.* 88:1034–1038.
15. Cohn, S. M., T. C. Simon, K. A. Roth, E. H. Birkenmeier, and J. I. Gordon. 1992. Use of transgenic mice to map *cis*-acting elements in the intestinal fatty acid binding protein gene (*Fabpi*) that control its cell lineage-specific and regional patterns of expression along the duodenal-colonic and crypt-villus axes of the gut epithelium. *J. Cell Biol.* 119:27–44.
16. DeCaprio, J. A., J. W. Ludlow, J. Figge, J.-Y. Shew, C. M. Huang, W.-H. Lee, E. Marsilio, E. Paucha, and D. M. Livingston. 1988. SV40 large tumor antigen forms a specific complex with the product of the retinoblastoma susceptibility gene. *Cell.* 54:275–283.
17. D'Emilia, J. C., B. Mathey-Prevot, K. Jaros, B. Wolf, G. Steele, Jr., and I. C. Summerhayes. 1991. Preneoplastic lesions induced by *myc* and *src* oncogenes in a heterotopic rat colon. *Oncogene.* 6:303–309.
18. Diller, L., J. Kassel, C. E. Nelson, M. A. Gryka, G. Litwak, M. Gebhardt, B. Bressac, M. Ozturk, S. J. Baker, and B. Vogelstein. 1990. p53 functions as a cell cycle control protein in osteosarcomas. *Mol. Cell Biol.* 10:5772–5781.
19. Dobbelstein, M., A. K. Arthur, S. Dehde, K. van Zee, A. Dickmanns, and E. Fanning. 1992. Intracistronic complementation reveals a new function of SV40 T antigen that co-operates with Rb and p53 binding to stimulate DNA synthesis in quiescent cells. *Oncogene.* 7:837–847.
20. Donehower, L. A., M. Harvey, B. L. Slagle, M. J. McArthur, C. A. Montgomery, Jr., J. S. Butel, and A. Bradley. 1992. Mice deficient for p53 are developmentally normal but susceptible to spontaneous tumours. *Nature (Lond).* 356:215–221.
21. El-Deiry, W. S., S. E. Kern, J. A. Pietenpol, K. W. Zinzler, and B. Vogelstein. 1992. Definition of a consensus binding site for p53. *Nature Genet.* 1:45–49.
21*a*. Falk, P., K. A. Roth, and J. I. Gordon. 1993. Lectins are sensitive tools for defining the differentiation programs of epithelial cell lineages in the developing and adult mouse gastrointestinal tract. *Am. J. Physiol.: Gastrointest. & Liver. Physiol.* In press.
22. Farmer, G., J. Bargonetti, H. Zhu, P. Friedman, R. Prywes, and C. Prives. 1992. Wild-type p53 activates transcription *in vitro*. *Nature (Lond.).* 358:83–86.
23. Fearon, E. R., S. R. Hamilton, and B. Vogelstein. 1987. Clonal analysis of human colorectal tumors. *Science (Wash. DC).* 238:193–197.
24. Fearon, E. R., K. R. Cho, J. M. Nigro, S. E. Kern, J. W. Simons, J. M. Ruppert, S. R. Hamilton, A. C. Preisinger, G. Thomas, K. W. Kinzler, and B. Vogelstein. 1990. Identification of a chromosome 18q gene that is altered in colorectal cancers. *Science (Wash. DC).* 247:49–56.
25. Forrester, K., C. Almoguera, K. Han, W. E. Grizzle, and M. Perucho. 1987. Detection of high incidence of K-*ras* oncogenes during human colon tumorigenesis. *Nature (Lond.).* 327:298–303.
26. Fuhlbrigge, R. C., S. M. Fine, E. R. Unanue, and D. D. Chaplin. 1988. Expression of membrane interleukin 1 by fibroblasts transfected with murine pro-interleukin 1 alpha cDNA. *Proc. Natl. Acad. Sci. USA.* 85: 5649–5653.
27. Funk, W. D., D. T. Pak, R. H. Karas, W. E. Wright, and J. W. Shay. 1992. A transcriptionally active DNA-binding site for human p53 protein complexes. *Mol. Cell Biol.* 12:2866–2871.
28. Ginsberg, D., F. Mechta, M. Yaniv, and M. Oren. 1991. Wild-type p53 can down-modulate the activity of various promoters. *Proc. Natl. Acad. Sci. USA.* 88:9979–9983.
29. Goodrich, D. W., N. P. Wang, Y.-W. Qian, E. Y.-H. P. Lee, and W.-H. Lee. 1991. The retinoblastoma gene product regulates progression through the G1 phase of the cell cycle. *Cell.* 67:293–302.
30. Gordon, J. I., G. H. Schmidt, and K. A. Roth. 1992. Studies of intestinal stem cells using normal, chimeric, and transgenic mice. *FASEB (Fed. Am. Soc. Exp. Biol.) J.* 6:3039–3050.
31. Griffiths, D. F. R., S. J. Davies, D. Williams, G. T. Williams, and E. D. Williams. 1988. Demonstration of somatic mutation and colonic crypt clonality by X-linked enzyme histochemistry. *Nature (Lond.).* 333: 461–466.
32. Groden, J., A. Thliveris, W. Samowitz, M. Carlson, L. Gelbert, H. Albertsen, G. Joslyn, J. Stevens, L. Spirio, M. Robertson, L. Sargent, K. Krapcho, E. Wolff, R. Burt, J. P. Hughes, J. Warrington, J. McPherson, J. Wasmuth, D. Le Paslier, H. Abderrahim, D. Cohen, M. Leppret, and R. White. 1991. Identification and characterization of the familial adenomatous polyposis coli gene. *Cell.* 66:589–600.
33. Hansbrough, J. R., D. M. Lublin, K. A. Roth, E. A. Birkenmeier, and J. I. Gordon. 1991. Expression of a liver fatty acid binding protein/human decay-accelerating factor/HLA-B44 chimeric gene in transgenic mice. *Am. J. Physiol.* 260:G929–G939.
34. Hauft, S. M., S. H. Kim, G. H. Schmidt, S. Pease, S. Rees, S. Harris, K. A. Roth, J. R. Hansbrough, S. M. Cohn, D. J. Ahnen, N. A. Wright, R. A. Goodlad, and J. I. Gordon. 1992. Expression of SV-40 T antigen in the small intestinal epithelium of transgenic mice results in proliferative changes in the crypt and reentry of villus-associated enterocytes into the cell cycle but has no apparent effect on cellular differentiation programs and does not cause neoplastic transformation. *J. Cell Biol.* 117:825–839.
35. Hermiston, M. L., C. B. Latham, J. I. Gordon, and K. A. Roth. 1992. Simultaneous localization of six antigens in single sections of transgenic mouse intestine using a combination of light and fluorescence microscopy. *J. Histochem. Cytochem.* 40:1283–1290.
36. Hogan, B., F. Costantini, and E. Lacy. 1986. Manipulating the Mouse Embryo: A Laboratory Manual. Cold Spring Harbor Laboratory Press, Cold Spring Harbor, NY. 1–315.
37. Hunter, T. 1991. Cooperation between oncogenes. *Cell.* 64:249–270.
38. Kastan, M. B., Q. Zhan, W. S. El-Deiry, F. Carrier, T. Jacks, W. V. Walsh, B. S. Plunkett, B. Vogelstein, and A. J. Fornace, Jr. 1992. A mammalian cell cycle checkpoint pathway utilizing p53 and *GADD45* is defective in ataxia-telangiectasia. *Cell.* 71:587–597.
39. Kedinger, M., P. M. Simon-Assmann, B. Lacroix, A. Marxer, H. P. Hauri, and K. Haffen. 1986. Fetal gut mesenchyme induces differentiation of cultured intestinal endodermal and crypt cells. *Dev. Biol.* 113:474–483.

40. Kedinger, M., P. Simon-Assmann, E. Alexandre, and K. Haffen. 1987. Importance of a fibroblastic support of an *in vitro* differentiation of intestinal endodermal cells and for their response to glucocorticoids. *Cell Differ.* 20:171–182.
41. Kedinger, M., P. Simon-Assmann, F. Bouziges, and K. Haffen. 1988. Epithelial-mesenchymal interactions in intestinal epithelial differentiation. *Scand. J. Gasteroenterol.* 23:62–69.
42. Kern, S. C., K. W. Kinzler, A. Bruskin, D. Jarosz, P. Friedman, C. Prives, and B. Vogelstein. 1991. Identification of p53 as a sequence-specific DNA-binding protein. *Science (Wash. DC).* 252:1708–1711.
43. Kinzler, K. W., M. C. Nilbert, L.-K. Su, B. Vogelstein, T. M. Bryan, D. B. Levy, K. J. Smith, A. C. Preisinger, P. Hedge, and D. McKechnie. 1991. Identification of FAP locus genes from chromosome 5q21. *Science (Wash. DC).* 253:661–665.
44. Kinzler, K. W., M. C. Nilbert, B. Vogelstein, T. M. Bryan, D. B. Levy, K. J. Smith, A. C. Preisinger, S. R. Hamilton, P. Hedge, A. Markham, M. Carlson, G. Joslyn, J. Groden, R. White, Y. Miki, Y. Miyoshi, I. Nishisho, and Y. Nakamura. 1991. Identification of a gene located at chromosome 5q21 that is mutated in colorectal cancers. *Science (Wash. DC).* 251:1366–1370.
45. Kuerbitz, S. J., B. S. Plunkett, W. V. Walsh, and M. B. Kastan. 1992. Wild-type p53 is a cell cycle checkpoint determinant following irradiation. *Proc. Natl. Acad. Sci. USA.* 89:7491–7495.
46. Lavigueur, A., V. Maltby, D. Mock, J. Rossant, T. Pawson, and A. Bernstein. 1989. High incidence of lung, bone, and lymphoid tumors in transgenic mice overexpressing mutant alleles of the p53 oncogene. *Mol. Cell. Biol.* 9:3982–3991.
47. Leder, A., A. Kuo, R. D. Cardiff, E. Sinn, and P. Leder. 1990. v-Ha-*ras* transgene abrogates the initiation step in mouse skin tumorigenesis: Effects of phorbol esters and retinoic acid. *Proc. Natl. Acad. Sci. USA.* 87:9178–9182.
48. Lee, Y. C., S. L. Asa, and D. J. Drucker. 1992. Glucagon gene 5′-flanking sequences direct expression of Simian Virus 40 large T antigen to the intestine, producing carcinoma of the large bowel in transgenic mice. *J. Biol. Chem.* 267:10705–10708.
49. Lin, D., M. T. Shields, S. J. Ullrich, E. Appella, and W. E. Mercer. 1992. Growth arrest induced by wild-type p53 protein blocks cells prior to or near the restriction point in late G_1 phase. *Proc. Natl. Acad. Sci. USA.* 89:9210–9214.
50. Lu, X., S. H. Park, T. C. Thompson, and D. P. Lane. 1992. *ras*-induced hyperplasia occurs with mutation of p53, but activated *ras* and *myc* together can induce carcinoma without p53 mutation. *Cell.* 70:153–161.
51. McCoy, M. S., C. I. Bargmann, and R. A. Weinberg. 1984. Human colon carcinoma Ki-*ras*2 oncogene and its corresponding proto-oncogene. *Mol. Cell. Biol.* 4:1577–1582.
52. Mercer, W. E., M. T. Shields, M. Amin, G. J. Sauve, E. Appella, J. W. Romano, and S. J. Ullrich. 1990. Negative growth regulation in a glioblastoma tumor cell line that conditionally expresses human wild-type p53. *Proc. Natl. Acad. Sci. USA.* 86:8763–8767.
53. Milner, J., and E. A. Medcalf. 1991. Cotranslation of activated mutant p53 with wild-type drives the wild-type p53 protein into the mutant conformation. *Cell.* 65:765–774.
54. Moore, M., A. K. Teresky, A. J. Levine, and M. Seiberg. 1992. p53 mutations are not selected for in Simian Virus 40 T-antigen-induced tumors from transgenic mice. *J. Virol.* 66:641–649.
55. Moser, A. R., H. C. Pitot, and W. F. Dove. 1990. A dominant mutation that predisposes to multiple intestinal neoplasia in the mouse. *Science (Wash. DC).* 247:322–324.
56. Moser, A. R., W. F. Dove, K. A. Roth, and J. I. Gordon. 1992. The *Min* (multiple intestinal neoplasia) mutation: its effect on gut epithelial cell differentiation and interaction with a modifier system. *J. Cell Biol.* 116:1517–1526.
57. Peltomäki, P., L. A. Aaltonen, P. Sistonen, L. Pylkkänen, J.-P. Mecklin, H. Järvinen, J. S. Green, J. R. Jass, J. L. Weber, F. S. Leach, G. M. Petersen. S. R. Hamilton, A. de la Chapelle, and B. Vogelstein. 1993. Genetic mapping of a locus predisposing to human colorectal cancer. *Science (Wash. DC).* 260:810–812.
58. Potten, C. S., and M. Loeffler. 1990. Stem cells: attributes, cycles, spirals, pitfalls and uncertainties. Lessons for and from the crypt. *Development (Camb.).* 110:1001–1020.
59. Powell, S. M., N. Zilz, Y. Beazer-Barclay, T. M. Bryan, S. R. Hamilton, S. N. Thibodeau, B. Vogelstein, and K. W. Kinzler. 1992. *APC* mutations occur early during colorectal tumorigenesis. *Nature (Lond.).* 359: 235–237.
60. Roth, K. A., and J. I. Gordon. 1990. Spatial differentiation of the intestinal epithelium: analysis of enteroendocrine cells containing immunoreactive serotonin, secretin and substance P in normal and transgenic mice. *Proc. Natl. Acad. Sci. USA.* 87:6408–6412.
61. Roth, K. A., J. M. Hertz, and J. I. Gordon. 1990. Mapping enteroendocrine cell populations in transgenic mice reveals an unexpected degree of complexity in cellular differentiation within the gastrointestinal tract. *J. Cell Biol.* 110:1791–1801.
62. Rubin, D. C., E. Swietlicki, K. A. Roth, and J. I. Gordon. 1992. Use of fetal intestinal isografts from normal and transgenic mice to study the programming of positional information along the duodenal-to-colonic axis. *J. Biol. Chem.* 265:15122–15133.
63. Sambrook, J., E. F. Fritsch, and T. Maniatis. 1989. Molecular Cloning. A Laboratory Manual. Cold Spring Harbor Laboratory Press, Cold Spring Harbor, NY.
64. Sandgren, E. P., C. J., Quaife, C. A. Pinkert, R. D. Palmiter, and R. L. Brinster. 1989. Oncogene-induced liver neoplasia in transgenic mice. *Oncogene.* 4:715–724.
65. SAS Institute Inc. 1989. SAS/STAT User's Guide, Version 6, Fourth Edition, Volume 1. SAS Institute Inc., Cary, NC.
66. Schmid, P., A. Lorenz, H. Hameister, and M. Montenarh. 1991. Expression of p53 during mouse embryogenesis. *Development (Camb.).* 113: 857–865.
67. Schmidt, G. H., M. M. Wilkinson, and B. A. J. Ponder. 1985. Cell migration pathway in the intestinal epithelium: an in situ marker system using mouse aggregation chimeras. *Cell.* 40:425–429.
68. Shaulsky, G., A. Ben-Ze'ev, and V. Rotter. 1990. Subcellular distribution of the p53 protein during the cell cycle of Balb/c 3T3 cells. *Oncogene.* 5:1707–1711.
69. Simon, T. C., K. A. Roth, and J. I. Gordon. 1993. Use of transgenic mice to map *cis*-acting elements in the liver fatty acid binding protein gene (*Fabpl*) that regulate its cell lineage-specific, differentiation-dependent, and spatial patterns of expression in the gut epithelium and in the liver acinus. *J. Biol. Chem.* 268:18345–18358.
70. Srinivasan, A., K. W. C. Peden, and J. M. Pipas. 1989. The large tumor antigen of simian virus 40 encodes at least two distinct transforming functions. *J. Virol.* 63:5459–5463.
71. Stürzbecher, H.-W., T. Maimets, P. Chumakov, B. Brain, C. Addison, V. Simanis, K. Rudge, R. Philp, M. Grimaldi, W. Court, and J. R. Jenkins. 1990. p53 interacts with $p34^{cdc2}$ in mammalian cells: Implications for cell cycle control and oncogenesis. *Oncogene.* 5:795–801.
72. Su, L.-K., K. W. Kinzler, B. Vogelstein, A. C. Preisinger, A. R. Moser, C. Luongo, K. A. Gould, and W. F. Dove. 1992. Multiple intestinal neoplasia caused by a mutation in the murine homolog of the APC gene. *Science (Wash. DC).* 256:668–670.
73. Sunter, J. P., D. R. Appleton, M. S. B. DeRodriguex, N. A. Wright, and A. J. Watson. 1979. A comparison of cell proliferation at different sites within the large bowel of the mouse. *J. Anat.* 129:883–842.
74. Sweetser, D. A., E. H. Birkenmeier, I. J. Klisak, S. Zollman, R. S. Sparkes, T. Mohandas, A. J. Lusis, and J. I. Gordon. 1987. The human and rodent intestinal fatty acid binding protein genes: a comparative analysis of their structure, expression, and linkage relationships. *J. Biol. Chem.* 262:16060–16071.
75. Sweetser, D. A., E. H. Birkenmeier, P. C. Hoppe, D. W. McKeel, and J. I. Gordon. 1988. Mechanisms underlying generation of gradients in gene expression within the intestine: an analysis using transgenic mice containing fatty acid binding protein-human growth hormone fusion genes. *Genes & Dev.* 2:1318–1332.
76. Taketo, M., A. C. Schroeder, L. E. Mobraaten, K. B. Gunning, G. Hanten, R. R. Fox, T. H. Roderick, C. L. Stewart, F. Lilly, C. T. Hansen, and P. A. Overbeek. 1991. FVB/N: an inbred mouse strain preferable for transgenic analyses. *Proc. Natl. Acad. Sci. USA.* 88:2065–2069.
77. Thibodeau, S. N., G. Bren, and D. Schaid. 1993. Microsatellite instability in cancer of the proximal colon. *Science (Wash. DC).* 260:816–819.
78. Trahair, J., M. Neutra, and J. I. Gordon. 1989. Use of transgenic mice to study the routing of secretory proteins in intestinal epithelial cells: analysis of human growth hormone compartmentation as a function of cell type and differentiation. *J. Cell Biol.* 109:3231–3242.
79. Tsubouchi, S., and C. P. Leblond. 1979. Migration and turnover of enteroendocrine and caveolated cells in the epithelium of the descending colon, as shown by radioautography after continuous infusion of ^{3}H-thymidine into mice. *Am. J. Anat.* 156:431–452.
80. Vogelstein, B., E. R. Fearon, S. R. Hamilton, S. E. Kern, A. C. Preisinger, M. Leppert, Y. Nakamura, R. Wjite, A. M. M. Smits, and J. L. Bos. 1988. Genetic alterations during colorectal-tumor development. *N. Engl. J. Med.* 319:525–532.
81. Wright, N. A., and M. Irwin. 1982. The kinetics of villus cell populations in the mouse small intestine: normal villi – the steady state requirement. *Cell Tissue Kinet.* 15:595–609.
82. Zambetti, G. P., D. Olson, M. Labow, A. J. Levine. 1992. A mutant p53 protein is required for maintenance of the transformed phenotype in cells transformed with p53 plus ras cDNAs. *Proc. Natl. Acad. Sci. USA.* 89:3952–3956.